The unique canopy structure, leaf morphology, and physiology of *Cornus drummondii*

by

Emmett Gregory Tooley

B.S., Fort Hays State University, 2020

A THESIS

submitted in partial fulfillment of the requirements for the degree

MASTER OF SCIENCE

Division of Biology
College of Arts and Sciences

KANSAS STATE UNIVERSITY
Manhattan, Kansas

2022

Approved by:

Major Professor
Jesse Nippert

Copyright

Abstract

Dense canopies are a key characteristic of clonal shrubs that enables their encroachment of mesic grasslands. These dense shrub canopies displace shade-intolerant grasses, resulting in reduced fire intensity and a gradual grassland-to-woodland transition. While the importance of dense canopies to clonal woody encroaching shrubs is well documented, the structure of their canopies and the mechanisms enabling clonal shrubs to facilitate dense canopies are not yet understood. To fill this knowledge gap, I investigated the canopy structure of *Cornus drummondii* (chapter 2) and the growth investment strategy enabling *C. drummondii* to facilitate dense canopies (chapter 3). In chapter 2, I measured the vertical distribution of leaves and light transmission in canopies of *C. drummondii* and their response to grazing and simulated browsing. In doing this, I also assessed the accuracy of two indirect methods of measuring leaf area index (LAI; the one-sided area of leaves per ground area). My results indicated that unbrowsed *C. drummondii* canopies had a mean LAI of ~8, exceeding the LAI of most temperate deciduous forests, and distributed half of their total LAI within a single, vertical 50 cm canopy section. Canopy sections with greater leaf density had lower light extinction rates compared to less dense sections. The evaluation of LAI in *C. drummondii* canopies with indirect methods revealed that an AccuPAR LP-80 ceptometer could accurately predict LAI in unbrowsed canopies, despite their high densities. However, the ceptometer overestimated the total LAI of browsed canopies by 46%. An Einscan Pro 2X Plus 3D handheld scanner had high precision at estimating the leaf area of individual ramets but became less accurate as leaf area increased. These results indicate that indirect LAI measurements can predict LAI in *C. drummondii* canopies despite the density of these canopies and varying rates of light extinction. In chapter 3, I

investigated the vertical distribution of leaf traits and physiology in relation to light availability across canopies of *C. drummondii* and the impact of simulated browsing and grazing. My results revealed that leaf mass per area (LMA) and leaf nitrogen per area (Na) varied ~3-fold across canopies, resulting in major differences in leaf physiological functioning. High LMA leaves had high photosynthetic capacity, while low LMA leaves used a novel strategy for maintaining light compensation points below ambient light levels. In response to browsing, *C. drummondii* modified its vertical allocation of leaf traits by increasing LMA and Na at lower canopy depths, leading to a greater photosynthetic capacity deeper in browsed canopies compared to control canopies. This response, along with greater light availability in browsed canopies, resulted in greater photosynthetic rates and resource-use efficiency deeper in browsed canopies compared to control canopies. My results suggest that the high LAI canopies of *C. drummondii* and its compensatory growth response to browsing are driven by the capacity of *C. drummondii* to dramatically alter leaf traits in response to light gradients—both spatially to achieve dense canopies and temporally to achieve compensatory growth. Together, these two studies provide a better understanding of the dense canopy structure of *C. drummondii* and the morphological and physiological mechanisms enabling *C. drummondii* to facilitate dense canopies and respond to grassland disturbance by browsing, both of which are key factors contributing to the successful encroachment of grasslands by *C. drummondii* and other woody encroaching species.

Table of Contents

List of Figures vii
List of Tables x
Acknowledgements xii
Dedication xiv
Chapter 1 - Introduction 1
LAI and Light Transmission 2
Morphology and Physiology 3
Objectives and hypothesis 4
References 6
Chapter 2 - The dense canopy structure and light environment of *Cornus drummondii*: a comparison of direct and indirect methods 10
Abstract 10
Introduction 11
Materials and Methods 16
Study Design 16
Statistical Methods 19
Results 20
Discussion 22
C. drummondii canopy structure and light environment 23
Comparison of methods 24
References 27
Tables and Figures 35
Chapter 3 - Intra-canopy leaf trait variation facilitates high leaf area index and compensatory growth in a clonal woody-encroaching shrub 47
Abstract 47
Introduction 48
Materials and Methods 51
Site Description 51
Study Design 52

Data Analysis 57
Results 58
Discussion 62
Vertical variation in leaf morphology and resource allocation in *C. drummondii*. 62
Influence of leaf morphology on leaf physiology and plant performance. 64
Influence of browsing and grazing on *C. drummondii* canopy dynamics. 65
Conclusions and Implications 68
References 70
Tables and Figures 82
Chapter 4 - Conclusion 91
References 95
Appendix A - Additional Information 96

List of Figures

Figure 2.1. Schematic illustrating the canopy depths (0, 50, 100, 150 cm), and canopy sections (0-50, 50-100, 100-150, 150-200 cm) used in the study. The 200 cm depth and 150-200 cm section were only used to account for a small number of leaves in estimates of total LAI with direct methods and were excluded from all comparisons with indirect methods. 40

Figure 2.2. Image illustrating the measurement of leaf inclination angle (θ_L). Panel (A) illustrates the first step of the process. Cartesian coordinates are defined for the scanned ramet, with the X-axis (red) representing the zenith. Panel (B) illustrates the θ_L measurement for an individual leaf. θ_L was derived from the total distance between point A and point B and the vertical distance (x-axis/zenith) between point A and point B. 41

Figure 2.3. (A) Cumulative LAI measured by canopy depth and (B) LAD of individual canopy sections measured with direct methods in *C. drummondii* canopies varying in herbivory treatments (browsed, control, grazed). Point and whiskers represent the mean ± standard error. 42

Figure 2.4. Density plot of the distribution of leaf inclination angles (θ_L) for leaves in canopies of *C. drummondii* varying by treatment. The dotted line denotes the mean θ_L for the specified treatment. 43

Figure 2.5. The coefficient of light extinction (*k*) from individual canopy sections varying by (A) Leaf area density, (B) depth, and (C) treatment. Point and whiskers represent the mean ± standard error of measurements. 44

Figure 2.6. Linear regression models of the relationships between direct and indirect measurements of the variables (A) the coefficient of light extinction, (B) cumulative LAI, (C) cumulative LAI varying by depth, (D) ramet leaf area (3D scanner), (E) LAD of canopy sections (F) LAD of canopy sections varying by treatment. The dotted red line in plots A, B, D, and E denotes a 1:1 ratio between the direct and indirect method. 45

Figure 2.7. (A) The clumping index for individual canopy sections varying by depth, and (B) the clumping index for entire canopies of *C. drummondii* varying by treatment. 46

Figure 3.1. (A) A large island of *C. drummondii* with a dense canopy on watershed K4A at Konza Prairie Biological Station, Manhattan, Kansas. The growth form of *C. drummondii* consists of dense clonal patches of interconnected ramets termed “islands”. (B) Diagram

showing a cross section through the center of a *C. drummondii* island illustrating its growth form and my sampling locations. Black circles represent the measurement location for each canopy depth. Diagram credit: *C. drummondii* island animation by Emily Wedel. Photo by Rachel Keen. 86

Figure 3.2. (A) LAI and (B) PAR measured in *C. drummondii* canopies at varying canopy depths (0 cm, 50 cm, 100 cm, and 150 cm) and herbivory treatments (browsed, control, grazed). Point and whiskers represent the mean ± standard error of the one sampling period for LAI, and the mean ± standard error for all four sampling periods for PAR. 87

Figure 3.3. (A) LMA and (B) N_a of leaves in *C. drummondii* canopies varying by canopy position (out, 0 cm, 50 cm, 100 cm, and 150 cm), herbivory treatment (browsed, control, and grazed), and sampling period (6/4/, 7/1, 8/1, 9/5). Point and whiskers represent the mean ± standard error. 88

Figure 3.4. C:N ratio of leaves varying by depth (A) and date (B), and %N of leaves varying by depth (C) and date (D). Point and whiskers represent the mean ± standard error. 89

Figure 3.5. (A) Ambient photosynthetic rates, (B) photosynthetic nitrogen-use efficiency, and (C) intrinsic water-use efficiency of leaves in *C. drummondii* canopies varying by canopy position (out, 0 cm, 50 cm, 100 cm, and 150 cm), herbivory treatment (browsed, control, and grazed), and sampling period (6/4, 7/1, 8/1, 9/5). Point and whiskers represent the mean ± standard error. 90

Figure A.1. C:N ratio of leaves varying by treatment, (B) %N of leaves varying by treatment, (C) iWUE of leaves varying by treatment, and (D) leaf $\delta^{13}C$ varying by treatment. Point and whiskers represent the mean ± standard error. 96

Figure A.2. $\delta^{13}C$ of leaves in *C. drummondii* canopies varying by canopy position (out, 0 cm, 50 cm, 100 cm, and 150 cm) and sampling period (6/4/, 7/1, 8/1, 9/5). Point and whiskers represent the mean ± standard error. 97

Figure A.3. Pearsons matrices for leaf morphological and physiological parameters sampled across the growing season. For each bivariate comparison, pearsons correlation coefficients (r) are given for the entire growing season (grey), the 6/4 sampling period (black), the 7/1 sampling period (red), the 8/1 sampling period (gold/yellow), and the 9/5 sampling period (green). Correlations with P-values < 0.05 are represented by an asterisk (*), P-value < 0.01

are represented by two asterisks (**), and P-values < 0.001 are represented by three asterisks (***). 98
Figure A.4. Pearsons matrices for leaf morphological parameters from leaves used in the *A*-c_i and light response curves, and physiological parameters derived from the *A*-c_i and light response curves. Correlatiosn with P-values < 0.05 are represented by an asterisk (*), P-value < 0.01 are represented by two asterisks (**), and P-values< 0.001 are represented by three asterisks (***). 99

List of Tables

Table 2.1. ANOVA results summarizing the effects of the categorical predictor variables on the response variables. All significant effects ($p<0.05$) are denoted with an asterisk (*). Abbreviations: LAI = leaf area index; LAD = leaf area density; *k* = coefficient of light extinction; θ_L = leaf inclination angle; Ω = clumping index. 35

Table 2.2. Summary of the AICc model selection for variables dealing with canopy structure using direct measurements. An asterisk (*) denotes the best fit models whose significance are further evaluated in Table 3. Abbreviations: *k* = coefficient of light extinction; LAD = leaf area density; θ_L = leaf inclination angle. 36

Table 2.3. ANOVA results for variables measured using direct methods in best fit regression models. All significant effects ($p<0.05$) are denoted with an asterisk (*). Abbreviations: *k* = coefficient of light extinction; LAD = leaf area density. 37

Table 2.4. Summary of the AICc model selection for variables dealing with the relationship between direct and indirect measurements. An asterisk (*) denotes the selected best fit models and the comparisons between direct and indirect methods whose significance are further evaluated in Table 5. Abbreviations: LAI = leaf area index; LAI_e = leaf area index measured with a ceptometer; LAD = Leaf area density; LAD_{cept} = leaf area density measured with a ceptometer; *k* coefficient of light extinction; k_{cept} = coefficient of light extinction measured with a ceptometer; LA = leaf area of ramet; LA_{3D} = leaf area of ramet measured with a 3D handheld scanner. 38

Table 2.5. ANOVA results for best fit regression models and models of individual comparisons dealing with the relationship between direct and indirect methods. All significant effects ($p<0.05$) are denoted with an asterisk (*). Abbreviations: LAI = leaf area index; LAI_e = leaf area index measured with a ceptometer; LAD = Leaf area density; LAD_{cept} = leaf area density measured with a ceptometer; *k* coefficient of light extinction; k_{cept} = coefficient of light extinction measured with a ceptometer; LA = leaf area of ramet; LA_{3D} = leaf area of ramet measured with a 3D handheld scanner. 39

Table 3.1. List of measured canopy and leaf traits with a brief description and units accompanying each variable. 82

Table 3.2. Summary of the mixed effects models analysis of variance. Table contains all variables that were measured at multiple periods throughout the growing season. All significant effects ($p<0.05$) are bold font and insignificant effects are normal font ($p>0.05$). Abbreviations: PAR = photosynthetically active radiation; LMA = leaf mass per area; N_a = leaf nitrogen per unit area; %N = percent leaf nitrogen; A_{net} = instantaneous photosynthetic rate at ambient light intensity; iWUE = intrinsic water-use efficiency; PNUE = photosynthetic nitrogen-use efficiency. 83

Table 3.3. Summary for the mixed effects model analysis of variance. Table summarizes response variables that were only measured during one period of the growing season. All significant effects ($p<0.05$) are bold font and insignificant effects are normal font ($p>0.05$). An asterisk is placed next to effects with marginal differences. Abbreviations: Vc_{max} = maximum velocity of carboxylation; J_{max} = maximum velocity of electron transport; LCP = light compensation point; R_d = dark respiration; Φ = apparent quantum yield; A_{2000} = photosynthetic rate at 2000 μmol m^{-2}-s^{-1}; LAI = leaf area index. 84

Table 3.4. Summary of means and standard errors for parameters extracted from the *A*-c_i and light response curves. See Table 1 for variable units. Abbreviations: Vc_{max} = maximum velocity of carboxylation; J_{max} = maximum velocity of electron transport; LCP = light compensation point; R_d = dark respiration; Φ = apparent quantum yield; A_{2000} = photosynthetic rate at 2000 μmol m^{-2}-s^{-1}. 85

Acknowledgements

I would like to thank all the people at Kansas State and Konza Prairie who made my master's degree enjoyable. First, I express my sincere gratitude to Jesse for taking me into his lab. Upon completing my undergraduate degree, one of my greatest desires was to continue studying plant ecophysiology and Jesse made that possible. Throughout my M.S. degree, Jesse was a great advisor and role model whose guidance enabled me to grow as a scientist. Some of the most important things I learned from Jesse were the habits that it takes to be a successful scientist and the collaborative nature of science, which I hope to emulate in my future scientific career. Jesse also does a good job of creating a fun casual atmosphere within the lab. I really enjoyed our lab cookouts at Konza, our field day, and all of our other lab get togethers.

I would also like to thank my incredible lab mates Seton Bachle, Rachel Keen, Emily Wedel, Ryan Donnelly, Shahla Mohammadi, and Anna Shats. I am grateful for your friendship over the past two years. Seton Bachle and Rachel Keen were mentors to me, helping me to get settled into my graduate degree, answering my questions in R, helping me gather data, and along with Jesse giving me guidance throughout the process of writing my first first-author paper. I would not be where I am today without them.

I would also like to thank Zak Ratajczak and Sonny Lee for taking the time to serve on my committee and to answer my questions, and Patrick O'Neal for teaching me to use the backhoe and for helping me every time something went wrong. Your assistance to me and other graduate students is greatly appreciated. I thank the undergraduate technicians Lauren Gill and Meghan Maine for your help with data collection and your work in the isotope lab. You are both incredibly hard workers. I would also like to thank my significant other, Anne-Sophie, and my family for your love and support.

Lastly, I would like to thank the Kansas State University Division of Biology, Konza Prairie Biological Station, LTER, the National Science Foundation, and the U.S. Department of Energy for funding and support to conduct research and complete my master's degree at Kansas State University.

Dedication

To my best friend and wife, Anne-Sophie.

Chapter 1 - Introduction

The tallgrass prairie of North America once covered 167-240 million acres, extending across the eastern Great Plains from Manitoba, Canada to the Gulf of Mexico (Smith 1992, Samson and Knopf 1994). Today, only 4-13% of the historic tallgrass prairie remains intact, with a majority of the remnant prairies existing within the Flint Hills ecoregion (Smith 1992, Samson et al. 2004). Much of the tallgrass prairie habitat was lost during the mid-19th to early-20th century due to the conversion of prairies to farmlands (Smith 2001). Today however, the major threat to the remaining tallgrass prairie habitats are losses and fragmentation by encroaching woody plant species (Archer 2017, Archer 1995, Ratajczak et al. 2012). In the Flint Hills ecoregion, woody plants can increase at rates of 1.4-2.7 % per year when fire is not frequent (Ratajczak et al. 2014).

In the past century, woody plants have expanded throughout grasslands worldwide in a phenomenon known as "woody plant encroachment", resulting in altered ecosystem structure and function, and losses of grassland biodiversity (Archer 1995, Stevens et al. 2017, Archer et al. 2017, Ratajczak et al. 2012, Sepp et al. 2021, Lett and Knapp 2003). Increased woody plant abundance in grasslands is the result of fire suppression, the loss of megafaunal browsers, elevated atmospheric [CO_2], intensification of grazing, and altered precipitation regimes; along with their interactions at local scales (Archer 2017, Briggs et al. 2002, Bond and Midgley 2000, Roques et al. 2001, Sankaran et al. 2005). Woody plant encroachment can occur across a range of climates, but typically occurs at higher rates with greater annual precipitation (Barger et al. 2011, Staver et al. 2011). While abundant research has investigated the drivers of woody encroachment, less research has investigated the mechanisms that enable individual species to encroach. In any given grassland, very few woody species have become aggressive encroachers

(Archer 2017). The handful of woody species responsible for woody plant encroachment have evolved various strategies to overcome grassland disturbance (Dantas and Pausas 2013, Lawes et al. 2011, Hoffmann and Solbrig 2003). In mesic grasslands, dense canopies are a key trait found in most of the dominant woody encroaching species. Dense canopies reduce light availability below canopies, displacing the shade-intolerant C_4 grasses that fuel fire, which results in fire suppression and drives the encroachment woody plants in grasslands. (Ratajczak et al. 2014, Lett and Knapp 2003, Osborne et al. 2018, Archer 2017).

Despite the importance of dense canopies to woody plant encroachment, very little research has investigated the vertical canopy structure and light transmission in canopies of woody encroaching species, or the mechanisms that enable woody encroaching species to achieve dense canopies.

LAI and Light Transmission

Leaf area index (LAI), defined as the total one-sided area of leaf tissue per unit ground surface area (Watson 1947), is a key variable in studies of plant canopy structure. LAI reflects the total area of foliage in the canopy enabling researchers to scale leaf level processes to the ecosystem level. Extensive research on LAI has focused on the relationship between LAI and light, due to the critical role of light to photosynthesis and the ability to predict LAI indirectly from light transmission (Bréda 2003, Watson 1958). Light in plant canopies decreases exponentially in response to LAI (Monsi and Saeki 1953, Monsi and Saeki 2005). However, the rate of exponential decrease in response to LAI, known as the coefficient of light extinction, varies between species and even within canopies due to differences in leaf angle distributions, zenith angle, leaf clumping, gap sizes, and distributions of woody materials (Yan et al. 2019, Zhang et al. 2014). When the rate of light extinction and the fraction of light transmitted are both

known, then LAI can be predicted based on a modified version of Beer-Lambert law developed by Monsi and Saeki (1953):

$$I = I_o e^{(-k \times LAI)}$$

Where I is the incident radiation above the canopy, I_o is the radiation transmitted through the canopy, and *k* is the coefficient of light extinction (Monsi and Saeki 1953, Monsi and Saeki 2005). This model has become the basis for indirect methods of measuring LAI from light transmission, which is one of the most common methods of measuring LAI (Bréda 2003). To measure LAI from light transmission, measurements of light intensity are made above the canopy and below the canopy to determine the fraction of light transmitted (Yan et al. 2019). Many optical instruments can estimate *k* from a few variables, but these methods must assume that foliage within the canopy is randomly dispersed in space (random leaf distribution), that the canopy has a spherical leaf angle distribution, and that woody materials do not have a significant effect on LAI (Yan et al. 2019). These assumptions are usually met in herbaceous species (Welles and Norman 1991, Lang and Yeqin 1986, Jonckheere et al. 2004), but are not always met in the large woody canopies of trees and shrubs, which can have significant impacts on the accuracy of indirect methods (Yan et al. 2019). Therefore, it is important that indirect methods are confirmed with direct measurements when the canopy structure of a species is not well understood (Zhang et al. 2014).

Morphology and Physiology

The increased height and high LAI of woody plants provide a greater capacity to compete for light compared to shorter herbaceous species. However, while large LAI values restrict light from shorter competitors, it can also have negative effects on the carbon gain of the plant through self-shading. As upper-canopy leaves intercept light, they decrease light availability for

leaves in the plants lower canopy. Therefore, increasing LAI becomes detrimental to a plant when the costs of leaf respiration and leaf production outweigh the benefits of additional light capture (Saeki 1960, Reich et al. 2009). For this reason, an optimal LAI exists for maximizing canopy photosynthesis relative to the physiology of the plant (Saeki 1960, Hikosaka 2005, Waring 1983). To deal with the effects of varying light availability across canopies, woody plants have evolved high plasticity in leaf morphology and physiology. In forest ecosystems, this is achieved by varying leaf morphological traits and nutrients in response to light availability to maximize the photosynthetic capacity of leaves in the high-light intensities of the upper canopy and minimize the light compensation point of leaves at low-light intensities in the lower canopy (Lewis et al. 2000, Walters et al. 1996).

Objectives and hypothesis

This thesis focuses on *Cornus drummondii* CA Mey, the predominant woody encroaching shrub in the Kansas tallgrass prairie. *C. drummondii* forms clonal shrub islands which spread radially through belowground rhizomatous stems (Ratajczak et al. 2011). The LAI of *C. drummondii* islands can exceed those of temperate deciduous forests, despite having heights of only 2-4 meters (Knapp et al. 2008, Ratajczak et al. 2011). These exceptionally dense canopies cause a displacement of native C4 grasses, resulting in fire extinction, and facilitating *C. drummondii*'s spread across the Kansas tallgrass prairie (Ratajczak et al. 2014). The central objective of this thesis was to investigate the canopy structure and growth investment strategy of *C. drummondii,* and their response to disturbance by browsing and grazing. In chapter 2, I investigated the investment strategy of *C. drummondii* by evaluating the vertical distribution of leaf morphology, physiology, and nutrients in canopies of *C. drummondii* to better understand the mechanisms that enable *C. drummondii* to facilitate dense canopies and a compensatory

growth response to browsing. In chapter 3, I investigate the vertical distribution of leaf area and the behavior of light in canopies of *C. drummondii*. In doing so, I evaluated the accuracy of two indirect methods of measuring LAI against direct measurements to give a better understanding of the limitations of indirect measurements in the uniquely dense canopies of *C. drummondii*.

References

Archer SR (1995) Tree-grass dynamics in a thornscrub savanna parkland: reconstructing the past and predicting the future. Ecoscience 2:83-89.

Archer SR, Andersen EM, Predick KI, Schwinning S, Steidl RJ, Woods SR (2017) Woody plant encroachment: causes and consequences. In *Rangeland systems* (pp. 25-84). Springer, Cham.

Barger NN, Archer S, Campbell J, Huang C, Morton J, Knapp AK (2011) Woody plant proliferation in North American drylands: A synthesis of impacts on ecosystem carbon balance. Journal of Geophysical Research: Biogeosciences 116:G00K07.

Bond, WJ, GF Midgley (2000) A proposed CO_2-controlled mechanism of woody plant invasion in grasslands and savannas. Global Change Biology 6:865–869.

Briggs JM, Knapp AK, Brock BL (2002) Expansion of woody plants in tall-grass prairie: A 15-year study of fire and fire-grazing interactions. American Midland Naturalist. 147:287–294.

Dantas VD, Pausas JG (2013) The lanky and the corky: fire-escape strategies in savanna woody species. Ecology 101:1265-72.

Hikosaka K. (2005) Leaf canopy as a dynamic system: ecophysiology and optimality in leaf turnover. Annals of Botany 95:521-53

Hoffmann WA, Solbrig OT (2003) The role of topkill in the differential response of savanna woody species to fire. Forest Ecology and Management 180:273-86.

Jonckheere I, Fleck S, Nackaerts K, Muys B, Coppin P, Weiss M, Baret F (2004) Review of methods for in situ leaf area index determination: Part I. Theories, sensors and hemispherical photography. Agricultural and Forest Meteorology 121:19-35.

Knapp A, Briggs J, Collins S, Archer S, Bret-Harte M, Ewers B, Peters D, Young D, Shaver G, Pendall E (2008) Shrub encroachment in North American grasslands: Shifts in growth form dominance rapidly alters control of ecosystem carbon inputs. Global Change Biology, 14:615–623.

Lang AR, Yueqin X (1986) Estimation of leaf area index from transmission of direct sunlight in discontinuous canopies. Agricultural and Forest Meteorology 37:229-43.

Lawes MJ, Adie H, Russell-Smith J, Murphy B, Midgley JJ (2011) How do small savanna trees avoid stem mortality by fire? The roles of stem diameter, height and bark thickness. Ecosphere 2:art42.

Lett M, Knapp A (2003) Consequences of shrub expansion in mesic grassland: resource alterations and graminoid responses. Journal Vegetation Science 14:487–496.

Lewis JD, McKane RB, Tingey DT, Beedlow PA (2000) Vertical gradients in photosynthetic light response within an old growth Douglas-fir and western hemlock canopy. Tree Physiology 20:447–456.

Monsi M, Saeki T (1953) Uber den Lichtfaktor in den Pflanzengesellschaften undseine Bedeutung fu¨r die Stoffproduktion. Japanese Journal of Botany 14:22–52.

Monsi M, Saeki T (2005) On the factor light in plant communities and its importance for matter production. Ann. Bot. 95: 549–567.

Osborne CP, Charles-Dominique T, Stevens N, Bond WJ, Midgley G, Lehmann CE (2018) Human impacts in African savannas are mediated by plant functional traits. New Phytologist 220:10-24.

Ratajczak Z, Nippert JB, Hartman JC, Ocheltree TW (2011) Positive feedbacks amplify rates of woody encroachment in mesic tallgrass prairie. Ecosphere 2:1–14.

Ratajczak Z, Nippert JB, Collins SL (2012) Woody encroachment decreases diversity across North American grasslands and savannas. Ecology 93:697–703.

Ratajczak Z, Nippert JB, Ocheltree TW (2014) Abrupt transition of mesic grassland to shrubland: evidence for thresholds, alternative attractors, and regime shifts. Ecology 95:2633– 2645.

Roques, K.G., T.G. O'Connor, and A.R. Watkinson. 2001. Dynamics of shrub encroachment in an African savanna: Relative influences of fire, herbivory, rainfall and density dependence. Journal of Applied Ecology 38:268–280.

Saeki T (1960) Interrelationships between leaf amount, light distribution and total photosynthesis in a plant community. Botanical Magazine Tokyo 73:55–63.

Samson F, Knopf F (1994) Prairie conservation in north america. BioScience 44:418-21.

Samson FB, Knopf FL, Ostlie WR (2004) Great Plains ecosystems: past, present, and future. Wildlife Society Bulletin 32:6-15.

Sankaran, M., N.P. Hanan, R.J. Scholes, J. Ratnam, D.J. Augustine, B.S. Cade, J. Gignoux, S.I. Higgins, X. Le Roux, F. Ludwig, and J. Ardo. 2005. Determinants of woody cover in African savannas. Nature 438: 846–849.

Sepp SK, Davison J, Moora M, Neuenkamp L, Oja J, Roslin T, Vasar M, Öpik M, Zobel M (2021) Woody encroachment in grassland elicits complex changes in the functional structure of above-and belowground biota. Ecosphere12:e03512.

Smith DD (1992) Tallgrass prairie settlement: Prelude to the demise of the tallgrass ecosystem. In *Proceedings of the Twelfth North American Prairie Conference* (pp. 195-199). University of Northern Iowa, Cedar Falls, IA.

Smith DD (2001) America's lost landscape: the tallgrass prairie. In *Proceedings of the Seventeenth North American Prairie Conference: Seeds for the future ~ Roots of the Past* (pp. 15-20). North Iowa Area Community College, Mason City, IA.

Staver AC, Archibald S, Levin SA (2011) The global extent and determinants of savanna and forest as alternative biome states. Science 334:230-2.

Stevens N, Lehmann CE, Murphy BP, Durigan G (2017) Savanna woody encroachment is widespread across three continents. Global change biology. 23:235-44.

Waring RH (1983) Estimating forest growth and efficiency in relation to canopy leaf area. Advances in Ecological Research 13:327-354

Walters M, Reich P (1996) Are shade tolerance, survival, and growth linked? Low light and nitrogen effects on hardwood seedlings. Ecology 77:841-853.

Watson DJ 1947. Comparative physiological studies in the growth of field crops. I. Variation in net assimilation rate and leaf area between species and varieties, and within and between years. Annals of Botany 11:41–76.

Welles JM, Norman JM (1991) Instrument for indirect measurement of canopy architecture. Agronomy Journal 83:818-25.

Yan G, Hu R, Luo J, Weiss M, Jiang H, Mu X, Xie D, Zhang W (2019) Review of indirect optical measurements of leaf area index: Recent advances, challenges, and perspectives. Agricultural and Forest Meteorology 265:390-411.

Zhang L, Hu Z, Fan J, Zhou D, Tang F (2014) A meta-analysis of the canopy light extinction coefficient in terrestrial ecosystems. Frontiers of Earth Science 8:599-609.

Chapter 2 - The dense canopy structure and light environment of *Cornus drummondii*: a comparison of direct and indirect methods

Abstract

Leaf area index (LAI) is a key variable for ecosystem modeling, exhibiting major controls over the fluxes of carbon, nutrients, water, and energy in an ecosystem. Indirect methods for measuring LAI are commonly used in the field of ecology to estimate the actual LAI values. However, indirect LAI measurements often deviate from actual LAI values, and more research is needed to evaluate the accuracy of indirect methods for different plant growth forms. In this project, I assessed the vertical canopy structure and leaf area index of *Cornus drummondii*, a clonal shrub with exceptionally dense canopies. I evaluated the accuracy of two indirect methods of measuring LAI, an AccuPAR LP-80 ceptometer and a handheld 3D scanner and compared them with direct LAI measurements using a leaf area meter. In addition, I also evaluated the strength of this relationship in response to grassland disturbance by simulated browsing and grazing, which may alter the structure of canopies. My results indicated that (1) the LAI of non-browsed *C. drummondii* canopies using direct methods averaged ~8.0 and distributed nearly half their LAI at the 50-100 cm canopy depth. The high leaf density within this canopy depth resulted in a lower coefficient of light extinction compared to the other depths. (2) Indirect measures of LAI using an AccuPAR LP-80 ceptometer produced accurate estimations for the total LAI of control and grazed canopies (7% overestimation and 1% underestimation) but overestimated the total LAI of browsed canopies by 46%. (3) Leaf area of individual ramets using a 3D scanner had a strong linear relationship with the actual leaf area of the ramets (R^2=0.86) but tended to

underestimate the leaf area from direct methods, especially at greater leaf area values. Overall, the study indicated that the AccuPAR LP-80 ceptometer was adequate for measuring LAI in dense clonal *C. drummondii* canopies when browsing was not present and the Einscan Pro 2x plus handheld 3D scanner was adequate for measuring leaf area of individual *C. drummondii* ramets. This study also highlights the impact of browsing on the accuracy of indirect estimations of LAI.

Introduction

Leaf area index (LAI), defined as the total one-sided area of leaf tissue per unit ground surface area (Watson 1947), is a key canopy trait driving the extinction of light, the exchange of water and CO_2, and plant primary production (Welles 1990, Bréda 2003, Running and Coughlan 1988). LAI represents the total amount of foliage within a canopy and enables the scaling of leaf level processes to the plant and ecosystem level (Running and Coughlan 1988). As such, LAI is one of the most valuable and widely used measurements in the field of ecology and has fostered extensive research on indirect methods of predicting LAI at varying scales (Yan et al. 2019, Bréda 2003).

The most accurate method of measuring LAI is to directly harvest leaves from sub-sections of a canopy and measure leaf area for each leaf individually using a leaf area meter or similar instrument (Bréda 2003). However, this approach can be tedious and time consuming and is not reasonable for larger canopies. For this reason, indirect methods of measuring LAI are commonly used. A widely used indirect method is the gap fraction method (or optical method) which estimates LAI from light transmission using optical sensors such as plant canopy analyzers and hemispherical photography (Yan et al. 2019, Bréda 2003). The gap fraction

method is based on the relationship between foliage and light extinction and can be quantified using an expanded version of Beer-Lambert law developed by Monsi and Saeki (1953):

$$I = I_o e^{(-k \times LAI)}$$

Where I is the incident radiation above the canopy, I_o is the radiation transmitted through the canopy, and *k* is the rate that light is extinguished in response to foliage, known as the coefficient of light extinction. *k* is a function of leaf angle distribution, and leaf-azimuth angle (Yan et al. 2019). Extensive research has investigated methods of evaluating k, which have become the basis for optical methods (Bréda 2003, Campbell 1986, Smith et al. 1991). To measure LAI using a plant canopy analyzer, measurements of incident radiation are made above or beside the canopy and transmitted radiation is measured below the canopy. From this, LAI is estimated based on the light interception along with an estimation of *k* (Yan et al. 2019). Using this method, plant canopy analyzers can successfully estimate LAI for many smaller plant species (Welles and Norman 1991, Lang and Yeqin 1986, Jonckheere et al. 2004). However, optical methods assume that elements of a canopy are randomly dispersed in space (random leaf distribution) and that the canopy has a spherical leaf angle distribution, as both of these factors are not readily measured (Yan et al. 2019, Bréda 2003). In larger tree and shrub species, these assumptions are not often met and can influence the accuracy of indirect methods (Yan et al. 2019, Bréda 2003). Canopies that do not exhibit random leaf distributions are prone to underestimation (clumped distribution) or overestimation (regular distribution) of LAI by optical methods (Ryu et al. 2010, Chen et al. 1996, Decagon Devices 2004). Indirect measurements are also affected by woody components of the canopy and their distributions (Chen 1996, Grower et al. 1999, Yan et al. 2019). This is typically evaluated using the wood-to-total area ratio (α) of a

canopy which can cause a significant overestimation of LAI by indirect methods as α increases (Chen 1996, Smolander and Stenburg 1996, Pokorný and Marek 2000).

While direct methods of measuring LAI are the best representation of the area of leaves in the canopy, LAI measurements based on gap fraction methods are a better representation of the area of plant material intercepting light and has therefore been called the "effective leaf area index" (LAI_e). The difference between the actual LAI and the area of LAI intercepting light (LAI_e), is calculated as:

$$LAI_e = \text{LAI} \times \Omega$$

Where Ω is the clumping index of a canopy (Black et al. 1991, Nilson et al. 1971, Chen et al. 1991, Fang 2021). Ω represents the difference between the actual LAI and effective LAI of the canopy. When $\Omega = 1$, then LAI and LAI_e are in unity, but in clumped canopies when $\Omega < 1$, then LAI_e is less than LAI, and in over-dispersed canopies when $\Omega > 1$, LAI_e is greater than LAI. Clumping typically increases at greater LAI and leaf area density (LAD; LAI per unit canopy volume), and LAI_e values deviate from LAI, and contain more error (Fang et al 2021).

Recent advances in technology have led to the 3D modeling of plant canopies to evaluate canopy structural traits such as LAI (Mathews and Jensen 2013, Hopkinson et al. 2013, Omasa et al. 2007). These models are typically formed from 3D point clouds created using LiDAR, multispectral imagery, 3D scanners, and other forms of photogrammetry (Zheng and Moskal 2009). A point cloud is a set of data points in space representing an object. These points are collected from the surface of an object with each point containing a set of cartesian coordinates. After a 3D point cloud is created, it is often converted into 3D surfaces through surface reconstruction. In many cases, the LAI of plants derived from 3D point clouds can be highly accurate at predicting LAI (Arnó et al. 2013, Thapa et al. 2020, Wang and Fang 2020), but in

other cases 3D plant models have been shown to underestimate LAI. Underestimation is often the result of the occlusion effect, which is a major source of error in LAI estimations from point clouds (Béland et al. 2014, Jiang et al. 2021, Soma et al. 2020). The occlusion effect occurs when laser or light pulses are blocked by leaves, inhibiting the pulses from contacting leaves further along their path (Béland et al. 2014, Jiang et al. 2021). The occlusion effect typically becomes more significant at greater leaf area density (Soma et al. 2020, Jiang et al. 2021). Underestimation of LAI is also the result of the smoothing of the leaf edges during surface reconstruction, which causes the exclusion of the finer structure of the leaf edge (Thapa et al. 2018). Both sources of underestimation are the result from the quality of the point cloud and become less problematic with greater point density and a greater number of scanning locations (Jiang et al. 2021, Soma et al. 2020).

Throughout grasslands around the globe, woody plants have expanded in a phenomenon known as "woody plant encroachment" (Archer 1995, Stevens et al. 2017, Archer et al. 2017), resulting in decreased grassland plant diversity (Ratajczak et al. 2012), and altering the dynamics of water, carbon, nutrients, and light within the ecosystem (Archer et al. 2017). Due to the impact of woody plants on grassland ecosystems, there is an incentive to model woody plant encroachment in grasslands at larger scales, requiring accurate measures of LAI. In mesic grasslands, clonal island forming shrubs are some of the most aggressive encroaching species (Ratajczak et al. 2011). These shrubs form tightly packed clonal patches termed 'islands' with dense canopies. *Cornus drummondi* and *Morella cerifera* have LAI values of ~8 and ~10 despite having heights of only 2-5 meters (Knapp et al. 2008, Brantley and Young 2007, Tooley et al. in review). The dense canopies of island forming shrubs are a key factor contributing to their encroachment of grasslands (Ratajczak et al. 2011, Briggs et al. 2005). By reducing understory

light availability, dense canopies exclude shade-intolerant grassland plants, leading to the extinction of fire—the primary suppressor of woody plants in grasslands (Lett and Knapp 2003, Archer et al. 2017). This feedback ultimately enables the survival and spread of clonal shrub islands across the prairie (Lett and Knapp 2003, Ratajczak et al. 2011).

While the canopy structure, distribution of LAI, and its effects on LAI_e are well understood in tree species across many ecosystems, little research has investigated the dense canopies of clonal island forming shrubs responsible for grassland woody plant encroachment. This project investigated the distribution of foliage and light within canopies of *Cornus drummondii* in response to grazed, ungrazed, and simulated browsed conditions. I also evaluated the accuracy of indirect LAI measurements using a ceptometer, and a handheld 3D scanner against direct measurements using a leaf area meter. I hypothesize that (1) LAD measured using direct methods would remain high and relatively constant at all canopy depths and $\boldsymbol{\theta_L}$ would decrease with canopy depth leading to a decrease in *k* at lower canopy depths. (2) LAI_e measures using a AccuPAR LP-80 ceptometer would under-predict LAI at greater LAD due to greater leaf clumping, leading to an underprediction of the actual LAI of dense *C. drummondii* canopies in the control and grazed treatments, and an accurate prediction of LAI in the less dense canopies of the browsed treatment. (3) The 3D handheld scanner will be highly accurate at predicting LAI at lower leaf area values but deviate from this trend at larger leaf area values.

Materials and Methods

Study Design

This study was conducted during June and July of the 2020 growing season at Konza Prairie Biological Station (KPBS), a 3,487-ha native tallgrass prairie in the northern Flint Hills ecoregion of Northeast Kansas, USA. KPBS is divided into experimental watershed units, each with a prescribed burn treatment and grazing treatment. Both experimental watersheds in this study consisted of 4-year fire return intervals, which are heavily encroached by woody shrubs and sub-shrubs, containing the highest abundance of the shrubs *Cornus drummondii* (roughleaf dogwood), *Rhus glabra* (smooth sumac), *Prunus americana* (American plum), and the subshrub *Ceanothus americana* (New Jersey tea).

For this study, I evaluated the canopy structure of *C. drummondii*, the most abundant woody encroaching shrub in the Kansas tallgrass prairie. *C. drummondii* forms dense clonal shrub islands, containing ~10-40 stems per square meter (Wedel et al. 2021, O'Connor et al. 2020), that expand radially through clonal rhizomatous stems (Ratajczak et al. 2014, Heisler et al. 2004, Briggs et al. 2005). At maturity, *C. drummondii* shrub islands can have total LAI of ~8 despite having heights of only 2-4 meters (Knapp et al. 2008, Tooley et al. in review).

Two experimental watersheds at KPBS were used to evaluate the effects of my treatments (browsing, grazing, and their absence (control)) on *C. drummondii* canopy structure and indirect LAI measurements. Watershed K4A does not contain any large grazing mammals and was used for the browsed and control treatments. Ten distinct *C. drummondii* islands of similar height were randomly selected across watershed K4A and assigned to the control and browsed treatments (5 islands/treatment). *C. drummondii* islands in the control treatment ranged in height from 2.02 to 2.45 meters, and *C. drummondii* islands in the browsed treatment ranged

from 1.83 to 2.47 meters. For the grazed treatment, five distinct *C. drummondii* islands were selected on watershed unit N4D, a nearby watershed that has had a 4-year fire return interval for a similar amount of time to K4A (since the 1980's). However, unlike watershed K4A, watershed N4D has been grazed by American bison (*Bison bison*) continuously since 1992. *C. drummondii* islands in the grazed treatment had similar heights to the control and browsed treatment, ranging from 2.03 to 2.85 meters. While bison do not consume significant amounts of *C. drummondii*, the consumption of grasses by bison reduces fire intensity and spread, leading to greater survival and abundance of *C. drummondii* in grazed watersheds compared to ungrazed watersheds (Briggs et al. 2002).

LAI and light availability.

All measurements were made from the middle of June to early July of the 2020 growing season (~3 weeks). *C. drummondii* shrub islands were marked near their center in the area containing the tallest ramets. Indirect measures of PAR and LAI were measured around the marked area using an AccuPAR-LP-80 ceptometer. Measurements were taken in sunny conditions between the times of 12:00 and 15:00 CST across a vertical canopy gradient containing four canopy depths: 0 cm (the top of the tallest ramet), 50 cm, 100 cm, and 150 cm (**Figure 2.1**). For each LAI measurement, eight instantaneous measurements of PAR were taken and averaged directly outside the canopy and eight instantaneous measurements of PAR were taken around the marked area at a given canopy depth. Measurements were taken from four directions (two measurements per direction; 90-degree rotation between directions). LAI was calculated by the ceptometer from the averaged measurements.

To evaluate LAI directly, a one square meter quadrat was placed over the marked area near the center of the shrub island. All ramets within the quadrat were cut at ground level, placed

in water, and transported for direct measurements. A Licor LI-3100C leaf area meter was used for the direct measurements of leaf area index. The leaves from all the ramets in the quadrat were harvested in 50 cm vertical sections. This consisted of four canopy sections: 0-50 cm, 50-100 cm, 100-150 cm, and 150-200 cm (**Figure 2.1**). The height of the tallest ramet in the quadrat was considered the top of the canopy (0 cm depth). These sections mimicked the depths of the indirect LAI measurements, except a 150-200 cm depth was also included to account for a small number of leaves existing below the 150 cm depth. The leaves in the 150-200 cm depth were not included in comparisons between the direct and indirect methods or comparisons between the direct methods and PAR but were only included for estimates of total leaf area. The cumulative LAI was calculated at each canopy depth by adding the LAI of all sections above the given depth. Leaf area density (LAD) was calculated for each canopy section as the one-sided leaf area per unit of canopy volume. Additionally, I also determined the coefficient of light extinction (*k*) for each canopy section. *k* was calculated from the LAI of the section and the difference in PAR between the top and bottom of the section by reorganizing the Beer-Lambert law equation:

$$K = -\ln(\frac{I}{I_o}) \times \frac{1}{LAI}$$

These parameters were also evaluated indirectly with the ceptometer. To do this, canopy depths were converted to canopy sections. (0-50 cm, 50-100 cm, and 100-150 cm). The value of LAI and PAR for each canopy section was calculated by taking the difference in their value between the top and bottom of the section. In addition to these parameters, I also evaluated the canopy clumping index (Ω) for the entire canopy, and for individual canopy sections by dividing the LAI_e measured with the ceptometer by the LAI measured using direct methods.

3D handheld scanner

I also evaluated canopy structure using a 3D handheld scanner. Two large ramets from each quadrat were randomly selected and scanned using an Einscan Pro 2X Plus 3D handheld scanner to create a 3D point cloud of the ramet. EXScanPro-3.6.X.X software was used to convert point cloud data into a mesh model and then evaluate LAI and leaf inclination angle (θ_L). LAI was calculated as half the total area of the scan since a majority of the scan was leaf tissue. θ_L was defined as the angle between the leaf surface normal and the zenith (Ross 1981, Ryu et al. 2009), and was calculated by taking the ratio of the horizontal length of a leaf to the vertical length of a leaf. (Ryu et al. 2009, Pisek et al. 2013; **Figure 2.2**). θ_L was measured at varying canopy depths for ~30 leaves per island of *C. drummondii*.

Statistical Methods

All analysis was done in R version 4.0.2 (R Core Team 2020). To evaluate the response of direct cumulative LAI, direct LAD, canopy Ω and sectional Ω in response to depth, treatment, and other predictor variables, I used generalized linear models. An ANOVA was used to determine the significance of parameters in models. When only categorical variables were involved, a Tukey's HSD test was performed to make pairwise comparison if a significant effect was found ($\alpha < 0.05$). To evaluate all other relationships, a global model was created containing all predictor variables and all possible interaction terms. In cases where rank deficiency occurred, multiple global models were used for separate predictor variables. I also tested transformations using log and squared terms for response variables and predictor variables that are known to have non-linear relationships (example: PAR and LAI). For each generalized linear model, the best-fit model was selected based on the lowest AICc score and a difference of at least two units. AICc selection was done using the model selection tool 'dredge()' from the MuMIn package (Barton 2015). For each best fit model, an ANOVA was used to estimate the significance of

model parameters, and regression analysis was performed to determine the strength of the relationship between variables.

Results

Direct measures of canopy structure

In canopies of *C. drummondii,* cumulative LAI measured by direct methods varied by treatment, depth, and their interaction (**Table 2.1**). Cumulative LAI increased with canopy depth for all treatments (**Figure 2.3A**). Mean cumulative LAI of the entire canopy was ~8 in control and grazed treatments, and ~3.25 in the browsed treatment (**Figure 2.3A**). The distribution of LAI throughout the canopy, measured as LAD, varied by canopy depth, treatment, and their interaction (**Table 2.1**). In all treatments, LAD was concentrated at the 50-100 cm depth, decreasing significantly at both higher and lower canopy depths (**Figure 2.3b**) In control and browsed treatment canopies, LAD at the 50-100 cm section was more than double all other sections, containing roughly half the plants total LAI **(Figure 2.3b)**.

The distribution of leaf inclination angles (θ_L) in *C. drummondii* canopies varied between treatments, but no differences in θ were found by canopy depth. (**Table 2.1**). By treatment, the mean θ_L was similar between the browsed (42.6º) and grazed (40.0º) treatments, but smaller in the control treatment compared to the other two treatments (27.7º**; Figure 2.4**).

The coefficient of light extinction (*k*) varied between treatments and by canopy depth, but not their interaction (**Table 2.1**). *k* was greater in the browsed treatment compared to the grazed treatment, but neither the browsed nor grazed treatments differed significantly from the control treatment (**Figure 2.5c**). *k* also varied by canopy depth and was lowest at the 0-50 cm section compared to the other two sections (**Figure 2.5b**). Differences in *k* were also affected by LAD

(**Table 2.3**), and two best fit models containing LAD performed similarly at explaining differences in *k* based on AICc (**Table 2.2**). One best fit model included the parameters LAD and Depth (R^2=0.50, **Table 2.3**). This model revealed a decrease in *k* with increasing LAD for the 0-50 cm and 100-150 cm depths, but a consistently low *k* at the 50-100 cm depth. The other best fit model only included the log of LAD (R^2 = 0.41; **Table 2.2**). In this best fit model, *k* decreased exponentially with increasing LAD (**Figure 2.5a**).

Comparison of methods

The comparison between *k* calculated from indirect measures with a ceptometer (k_{cept}), and *k* calculated from direct measures using the leaf area meter for individual canopy sections revealed no relationship (R^2 = 0.062; **Table 2.5**; **Figure 2.6a**). Two best fit models were also used for the comparison of *k* and k_{cept}, one from a global model containing treatment and treatment* k_{cept} and one from a global model containing depth and depth*k_{cept} (**Table 2.4**). In the former global model, k_{cept} was not a significant factor and was not included in the best fit model. In the latter global model, the parameters k_{cept} and treatment were both included in the best fit model but explained very little variation in *k* (R^2 = 0.45; **Table 2.5**).

The comparison of direct cumulative LAI measurements (LAI) and indirect cumulative LAI measurements using a ceptometer (LAI_e) revealed a strong linear relationship with a slope of 0.945 (R^2=0.85; **Table 2.5**; **Figure 2.6b**). However, the best fit model for determining LAI also included an effect by treatment and an interaction between treatment and LAI_e (R^2=0.88; **Table 2.4**), causing the slope of the relationship between LAI and LAI_e to vary slightly between treatments **(Figure 2.6c)**. No significant difference occurred between the control and grazed treatments, and the slope of the two treatments were 0.855 and 1.112 (**Table 2.5**). However, the browsed treatment had had a slope of 0.614 (**Table 2.5**), resulting in an overestimation of the

actual LAI by the ceptometer in the browsed treatment (**Figure 2.6c)**. This trend was also seen in the canopy clumping index (Ω), which also varied by treatment, having a significantly greater Ω in the browsed treatment compared to the control and grazed treatments (**Figure 2.7b**; **Table 2.1**). Mean Ω of canopies in the control and grazed treatments were each close to ~1, while Ω of canopies in the browsed treatment had a mean of 1.46 (**Figure 2.7b**). Ω also varied significantly by depth for the evaluation of individual canopy sections, with a greater Ω in the 0-50 cm depth (**Figure 2.7a; Table 2.1**).

The parameters direct leaf area density (LAD) and indirect LAD using the ceptometer (LAD_{cept}) for individual canopy sections had a linear relationship of moderate strength (R^2=0.52; **Table 2.5**; **Figure 2.6e**). The best fit model for determining LAD included LAD_{cept} and treatment (R^2=0.61; **Table 2.4**). In the best fit model, the browsed treatment had a greater predicted LAD_{cept} at any given LAD value compared to the control and grazed treatments (**Figure 2.6f**, **Table 2.5**)

For the comparison of total leaf area of individual ramets using the 3D handheld scanner (LA_{3D}) with the total leaf area from direct measures using the leaf area meter (LA). The two methods had a strong linear relationship. (R^2= 0.86; **Table 2.5**), but the slope of this relationship was 1.305, leading to an underestimation of the actual leaf area by the 3D scanner especially as leaf area increased (**Figure 2.6d**)

Discussion

Indirect methods of measuring LAI have become the dominant form of measurement, ranging from optical instruments to LiDAR, and hyperspectral imaging from terrestrial, aerial, and satellite platforms (Zheng and Moskal 2009, Bréda 2003). However, plant canopy structure

can have substantial effects on the accuracy of these methods causing deviations from reality, but its effects are not often addressed (Fang et al. 2019, Fang et al. 2012, Pau et al. 2022). The objective of this study was to directly evaluate the vertical canopy structure of the clonal dense canopied shrub *C. drummondii* and its impact on two indirect methods of measuring LAI. My major findings revealed that an AccuPAR LP-80 ceptometer could accurately estimate LAI on grazed and ungrazed watersheds when simulated browsing (leaf removal) is absent, despite large vertical variation in *k* in *C. drummondii* canopies in response to varied canopy LAD. However, the AccuPAR LP-80 overestimated LAI by 46% in the presence of simulated browsing, casting doubt on the accuracy of its estimations in heavily browsed environments when calibration with direct measurements has not been done and canopy architecture is not known. 3D models created using the 3D handheld scanner tended to underestimate ramet leaf area and became more biased at larger leaf areas.

C. drummondii canopy structure and light environment

In the high LAI canopies of *C. drummondii*, I hypothesized that LAD measured using direct methods would remain constant, and θ_L would decrease with canopy depth leading to a decrease in the coefficient of light extinction (*k*) at lower canopy depths. However, my results indicated that θ_L did not vary with canopy depth, which is less common for tree species (Hutchinson et al. 1986, Niinemets 1998, Raabe et al. 2015, Chianucci et al. 2018, de Mattos et al. 2020), and supports the findings of Raabe et al. (2015) and Ryu et al. (2010) who found that tree species in open canopy ecosystems (savannahs & parks) do not typically vary θ_L by canopy depth. My findings also revealed that unbrowsed *C. drummondii* canopies had LAI values of ~8 and distributed nearly half their LAI in the 50-100 cm depth, resulting in significantly greater LAD values at this depth compared to the LAD of both lower and higher canopy depths. Greater

LAD corresponded with a lower coefficient of light extinction (*k*), and thus an overall lower *k* at the dense 50-100 cm depth. Decreased *k* with greater LAD supports the findings of Brown and Parker (1994), Zhang et al. (2014), Binkley et al. (2014), and Sampson and Allen (1998), and further suggests that light transmission in canopies is more complex than measuring above canopy and below canopy light and assuming a constant *k* value, which can bias plant and ecosystem models. (Zhang et al. 2014).

Comparison of methods

Indirect methods of measuring LAI based on optical methods rely on the assumption that leaves within the canopy are randomly dispersed and thus tend to underestimate the LAI of clumped canopies. This is especially true in dense canopies where LAI is concentrated leading to a greater LAD (Zhang et al. 2014). Therefore, I hypothesized that indirect LAI measurements with the ceptometer would under-predict LAI at greater LAD, leading to an under-prediction of the actual LAI for dense canopies of *C. drummondii* in the control and grazed treatments, and an accurate prediction of LAI in the less dense canopies of the browsed treatment. However, my results did not support this hypothesis. While the slope of the relationship between LAD and LAD_{cept} was less than one leading to an under-prediction of LAI at greater LAD, the strength of this relationship was not strong (R^2= 0.52) and did not hold up across depths. The clumping index for the 50-100 cm depth was close to 1.0, indicating that indirect LAI measures matched the actual LAI at the densest canopy depth. However, the 0-50 cm depth, containing a significantly lower LAD, had a clumping index of 1.52, overestimating LAI by 52%. I speculate that the high clumping factor at the 0-50 cm depth is due to leaves being over-dispersed at this canopy depth, and that increased clumping at the 50-100 cm depth brings the clumping index to 1.0.

Independent measures of LAI_e by the ceptometer accurately predicted the actual LAI for both control and grazed treatments but overestimated the LAI of the browsed treatment by 46%. The overestimation of LAI in browsed treatments could be due to a few factors. I speculate that the removal of leaves during browsing increased the ratio of wood to leaves in browsed canopies, which is a significant factor that can cause overestimation of LAI (Chen 1996, Yan et al. 2019, Whitford et al. 1995)

I also hypothesized that the 3D handheld scanner would show a very strong relationship with ramet leaf area, but it would deviate from this trend at larger leaf area values. My findings supported this hypothesis. 3D models created with the 3D handheld scanner tended to underestimate ramet leaf area and became more biased at larger leaf areas. This was likely the result of the occlusion effect (Béland et al. 2014, Jiang et al. 2021), since it was noticed on multiple occurrences that leaves in the centers of larger crowns were not readily scanned. 3D handheld scanners are not a reasonable method of evaluating LAI of larger tree species, but these instruments are promising for studies of plant structure and phenotyping for crops and smaller herbaceous species. The specific instrument used in this study (Einscan Pro 2X Plus) was very effective for evaluation of leaf area and its distributions, but it was noticed that branches and woody material woody material below 5 mm in diameter were not recorded by the scanner during the scanning process. Branch features such as branching angle, diameter, and length are often used in studies of plant canopy structure. Therefore, this specific instrument may not be useful for applications that evaluate the architecture of smaller branches.

In conclusion, the comparison of indirect LAI measurements using an AccuPAR LP-80 ceptometer and an Einscan Pro 2X Plus 3D handheld scanner with direct LAI measurements revealed that both methods were adequate for measuring LAI in unbrowsed *C. drummondii*

canopies without the need for adjustment using a calibration curve. However, in the presence of high intensity browsing, calibration is needed for accurate LAI estimates. The effect of browsing on LAI estimates has significant implications for savannah ecosystems with intact communities of browsing herbivores. In the North American Great Plains, populations of browsing herbivores including elk (*Cervus elaphus*), mule deer (*Odocoileus hemionus*), and pronghorn (*Antilocapra americana*) were largely extirpated in the late 19th century (Conard et al. 2006, Rickel 2005). Today, browser reintroductions have been proposed as an effective strategy for combating woody plant encroachment (Wilcox et al. 2021, O'Connor et al. 2020). In this scenario, browsers will likely have significant effects on LAI estimates causing an overestimation of indirect LAI with optical instruments. Therefore, LAI should be independently corroborated by direct methods for a given browsing intensity if indirect measurements are used. LAI estimates by 3D handheld scanners offer a novel approach for evaluating LAI and other canopy architectural traits at significantly lower cost than LiDAR scan stations. However, this method also results in an overestimation of LAI. Due to this, I suggest that species-specific calibration curves are used to account for this effect. Overall, this study indicates that both an AccuPAR LP-80 ceptometer and an Einscan Pro 2x plus handheld 3D scanner were adequate for measuring LAI in dense clonal *C. drummondii* canopies and highlights the negative effects that browsing can have on indirect estimations of LAI.

References

Archer SR (1995) Tree-grass dynamics in a thornscrub savanna parkland: reconstructing the past and predicting the future. Ecoscience 2:83-89.

Archer SR, Andersen EM, Predick KI, Schwinning S, Steidl RJ, Woods SR (2017) Woody plant encroachment: causes and consequences. In *Rangeland Systems* (pp. 25-84). Springer, Cham.

Bréda N (2003) Ground-based measurements of leaf area index: a review of methods, instruments and current controversies. Journal of Experimental Botany 54:2403–2417,

Barton K (2015) MuMIn: Multi-Model Inference. R package version 1.15.1. https://cran.r-project.org/web/packages/MuMIn/index.html

Béland M, Baldocchi DD, Widlowski JL, Fournier RA, Verstraete MM (2014) On seeing the wood from the leaves and the role of voxel size in determining leaf area distribution of forests with terrestrial LiDAR. Agricultural and Forest Meteorology 184:82-97.

Binkley D, Campoe OC, Gspaltl M, Forrester DI (2013). Light absorption and use efficiency in forests: why patterns differ for trees and stands. Forest Ecology and Management 288: 5–13

Black TA, Chen JM, Lee XH, Sagar RM (1991) Characteristics of shortwave and longwave irradiances under a douglas-fir forest stand. Canadian Journal of Forest Research 21:1020-1028.

Brantley ST, Young DR (2007) Leaf-area index and light attenuation in rapidly expanding shrub thickets. Ecology 88:524–530.

Briggs JM, Knapp AK, Brock BL (2002) Expansion of woody plants in tall-grass prairie: A 15-year study of fire and fire-grazing interactions. American Midland Naturalist 147:287–294.

Briggs JM, Knapp AK, Blair JM, Heisler JL, Hoch GA, Lett MS, McCarron JK (2005) An ecosystem in transition: causes and consequences of the conversion of mesic grassland to shrubland. BioScience 55:243-54.

Brown MJ, Parker GG (1994) Canopy light transmittance in a chronosequence of mixed-species deciduous forests." Canadian Journal of Forest Research 24:1694-1703.

Campbell GS, Norman JM (1989). The description and measurement of plant canopy structure. In *Plant canopies: their growth, form and function* (pp. 1–19) Cambridge University Press, Cambridge, England.

Campbell GS (1986) Extinction coefficients for radiation in plant canopies calculated using an ellipsoidal inclination angle distribution. Agricultural and Forest Meteorology 36:317-321.

Chen JM, Black TA, Adams RS (1991) Evaluation of hemispherical photography for determining plant area index and geometry of a forest stand. Agricultural and Forest Meteorology 56:129-143.

Chen JM (1996) Optically-based methods for measuring seasonal variation of leaf area index in boreal conifer stands. Agricultural and Forest Meteorology 80:135–163.

Chianucci F, Pisek J, Raabe K, Marchino L, Ferrara C, Corona P (2018) A dataset of leaf inclination angles for temperate and boreal broadleaf woody species. Annals of Forest Science 75:1-7.

Conard JM, Gipson PS, Peek M (2006) Historical and current status of Elk in Kansas. Pages 307–312 in *Prairie Invaders: Proceedings of the 20th North American Prairie Conference*. University of Nebraska Press, Lincoln, Nebraska, USA.

Decagon Devices (2004) AccuPAR PAR/LAI Ceptometer (model LP-80) Operator's Manual Version 1. 2, Pullman, WA, USA

de Mattos EM, Binkley D, Campoe OC, Alvares CA, Stape JL (2020) Variation in canopy structure, leaf area, light interception and light use efficiency among Eucalyptus clones. Forest Ecology and Management 463:118038.

Fang H, Wei S, Liang S. (2012) Validation of MODIS and CYCLOPES LAI products using global field measurement data. Remote Sensing of Environment 119:43-54.

Fang H, Zhang Y, Wei S, Li W, Ye Y, Sun T, Liu W (2019) Validation of global moderate resolution leaf area index (LAI) products over croplands in northeastern China. Remote Sensing of Environment 233:111377.

Fang H (2021) Canopy clumping index (CI): A review of methods, characteristics, and applications. Agricultural and Forest Meteorology. 303:108374.

Heisler JL, Briggs JM, Knapp AK, Blair JM, Seery A (2004) Direct and indirect effects of fire on shrub density and aboveground productivity in a mesic grassland. Ecology 85:2245-57.

Hopkinson C, Lovell J, Chasmer L, Jupp D, Kljun N, van Gorsel E (2013) Integrating terrestrial and airborne lidar to calibrate a 3D canopy model of effective leaf area index. Remote Sensing of Environment 136:301-14.

Hutchison BA, Matt DR, McMillen RT, Gross LJ, Tajchman SJ, Norman JM (1986) The architecture of a deciduous forest canopy in eastern Tennessee, USA. Ecology 1:635-46.

Jonckheere I, Fleck S, Nackaerts K, Muys B, Coppin P, Weiss M, Baret F (2004) Review of methods for in situ leaf area index determination: Part I. Theories, sensors and hemispherical photography. Agricultural and Forest Meteorology 121:19-35.

Jiang H, Hu R, Yan G, Cheng S, Li F, Qi J, Li L, Xie D, Mu X (2021) Influencing Factors in Estimation of Leaf Angle Distribution of an Individual Tree from Terrestrial Laser Scanning Data. Remote Sensing 13:1159.

Knapp A, Briggs J, Collins S, Archer S, Bret-Harte M, Ewers B, Peters D, Young D, Shaver G, Pendall E (2008) Shrub encroachment in North American grasslands: Shifts in growth form dominance rapidly alters control of ecosystem carbon inputs. Global Change Biology, 14:615–623.

Lang AR, Yueqin X (1986) Estimation of leaf area index from transmission of direct sunlight in discontinuous canopies. Agricultural and Forest Meteorology 37:229-43.

Lett M, Knapp A (2003) Consequences of shrub expansion in mesic grassland: resource alterations and graminoid responses. Journal Vegetation Science 14:487– 496.

Mathews AJ, Jensen JL (2013) Visualizing and quantifying vineyard canopy LAI using an unmanned aerial vehicle (UAV) collected high density structure from motion point cloud. Remote Sensing 5:2164-83.

Niinemets Ü (1998) Adjustment of foliage structure and function to a canopy light gradient in two co-existing deciduous trees. Variability in leaf inclination angles in relation to petiole morphology. Trees 12:446-51.

Nilson T (1971) A theoretical analysis of the frequency of gaps in plant stands. Agricultural and Forest Meteorology 8:25-38.

O'Connor RC, Taylor JH, Nippert JB (2020) Browsing and fire decreases dominance of a resprouting shrub in woody encroached grassland. Ecology 101:e02935.

Omasa K, Hosoi F, Konishi A (2007) 3D lidar imaging for detecting and understanding plant responses and canopy structure. Journal of Experimental Botany 58:881-98.

Pisek J, Sonnentag O, Richardson AD, Mõttus M (2013) Is the spherical leaf inclination angle distribution a valid assumption for temperate and boreal broadleaf tree species?. Agricultural and Forest Meteorology 169:186-94.

Pau S, Nippert JB, Slapikas R, Griffith D, Bachle S, Helliker BR, O'Connor RC, Riley WJ, Still CJ, Zaricor M (2022) Poor relationships between NEON Airborne Observation Platform data and field-based vegetation traits at a mesic grassland. Ecology 103:e03590.

Pokorný R, Marek MV (2000) Test of accuracy of LAI estimation by LAI-2000 under artificially changed leaf to wood area proportions. Biologia Plantarum 3:537-44.

Ratajczak Z, Nippert JB, Hartman JC, Ocheltree TW (2011) Positive feedbacks amplify rates of woody encroachment in mesic tallgrass prairie. Ecosphere 2:1-14.

Ratajczak Z, Nippert JB, Collins SL (2012) Woody encroachment decreases diversity across North American grasslands and savannas. Ecology 93:697–703.

Ratajczak Z, Nippert JB, Ocheltree TW (2014) Abrupt transition of mesic grassland to shrubland: evidence for thresholds, alternative attractors, and regime shifts. Ecology 95:2633–2645.

Rickel B (2005) Chapter 2: large native ungulates. In *General Technical Report RMRS-GTR-135 2* (pg 13-34). USDA Forest Service, Washington, D.C., USA.

Running SW, Coughlan JC (1988) A general model of forest ecosystem processes for regional applications I. Hydrologic balance, canopy gas exchange and primary production processes. Ecological Modelling 42:125-54.

Ryu Y, Nilson T, Kobayashi H, Sonnentag O, Law BE, Baldocchi DD (2010) On the correct estimation of effective leaf area index: Does it reveal information on clumping effects? Agricultural and Forest Meteorology 150:463-72.

Sampson DA, Allen HL (1998) Light attenuation in a 14-year-old loblolly pine stand as influenced by fertilization and irrigation. Trees 13:80-87

Smolander H, Stenberg P (1996) Response of LAI-2000 estimates to changes in plant surface area index in a Scots pine stand. Tree Physiology 16:345-9.

Smith WK, Knapp AK, Reiners WA (1989) Penumbral effects on sunlight penetration in plant communities. Ecology 70:1603-1609.

Smith FW, Sampson AD, Long NJ (1991) Comparison of leaf area index estimates from tree allometrics and measured light interception. Forest Science 37:1682–1688.

Smith NJ (1993) Estimating plant area index and light extinction coefficients in stands of Douglas-fir (Pseudotsuga Menziesii). Canadian Journal of Forest Research 23:317–321.

Stevens N, Lehmann CER, Murphy BP, Durigan G (2017) Savanna woody encroachment is widespread across three continents. Global Change Biology 23:235–244.

Thapa S, Zhu F, Walia H, Yu H, Ge Y (2018) A novel LiDAR-based instrument for high-throughput, 3D measurement of morphological traits in maize and sorghum. Sensors 18:1187.

Tooley EG, Nippert JB, Bachle S, Keen RM (in review) Intra-canopy leaf trait variation facilitates high leaf area index and compensatory growth in a clonal woody-encroaching shrub. Tree physiology.

Wang Y, Fang H (2020) Estimation of LAI with the LiDAR technology: A review. Remote Sensing 12:3457.

Watson DJ (1947) Comparative physiological studies in the growth of field crops. I. Variation in net assimilation rate and leaf area between species and varieties, and within and between years. Annals of Botany11:41–76.

Wedel E, Nippert JB, Hartnett D (2021) Fire and browsing interact to alter intra-clonal stem dynamics of an encroaching shrub in tallgrass prairie. Oecologia 196:1039–1048.

Welles JM (1990) Some indirect methods of estimating canopy structure. Remote Sensing Reviews 5:31-43.

Welles JM, Norman JM (1991) Instrument for indirect measurement of canopy architecture. Agronomy Journal 83:818-25.

Whitford KR, Colquhoun IJ, Lang AR, Harper BM (1995) Measuring leaf area index in a sparse eucalypt forest: a comparison of estimates from direct measurement, hemispherical photography, sunlight transmittance and allometric regression. Agricultural and Forest Meteorology 74:237-49.

Wilcox BP, Fuhlendorf SD, Walker JW, Twidwell D, Wu XB, Goodman LE, Treadwell M, Birt A (2021) Saving imperiled grassland biomes by recoupling fire and grazing: a case study from the Great Plains. Frontiers in Ecology and the Environment 20:179–186

Yan G, Hu R, Luo J, Weiss M, Jiang H, Mu X, Xie D, Zhang W. Review of indirect optical measurements of leaf area index: Recent advances, challenges, and perspectives. Agricultural and Forest Meteorology 265:390-411.

Yao J, Holt RD, Rich PM, Marshall WS (1999) Woody plant colonization in an experimentally fragmented landscape. Ecography 22:715-28.

Zhang L, Hu Z, Fan J, Zhou D, Tang F (2014) A meta-analysis of the canopy light extinction coefficient in terrestrial ecosystems. Frontiers of Earth Science 8:599-609.

Zheng G, Moskal LM (2009). Retrieving leaf area index (LAI) using remote sensing: theories, methods and sensors. Sensors 9:2719-45.

Tables and Figures

Table 2.1. ANOVA results summarizing the effects of the categorical predictor variables on the response variables. All significant effects ($p<0.05$) are denoted with an asterisk (*). Abbreviations: LAI = leaf area index; LAD = leaf area density; *k* = coefficient of light extinction; θ_L = leaf inclination angle; Ω = clumping index.

Response Variable	Predictor Variable	DF	F	P
LAI	Depth	4	69.7824	<0.001 *
	Treatment	2	39.0905	<0.001 *
	Depth*Treatment	8	4.3851	<0.001 *
LAD	Section Depth	3	43.8516	<0.001 *
	Treatment	2	16.9556	<0.001 *
	Depth*Treatment	6	4.1823	0.001845 *
k	Depth	2	4.5706	0.01746 *
	Treatment	2	3.7881	0.03272 *
	Depth*Treatment	4	1.0946	0.37492
θ_L	Treatment	2	23.842	<0.001 *
Canopy Ω	Treatment	2	4.7139	0.01451 *
Sectional Ω	Depth	2	3.2953	0.04920*
	Treatment	2	4.7585	0.01506 *
	Depth*Treatment	4	0.9821	0.43032

Table 2.2. Summary of the AICc model selection for variables dealing with canopy structure using direct measurements. An asterisk (*) denotes the best fit models whose significance are further evaluated in Table 3. Abbreviations: *k* = coefficient of light extinction; LAD = leaf area density; θ_L = leaf inclination angle.

Variable	Model	Model Parameters	AICc	R^2
k	Global	*k* = LAD + Depth + Treatment + LAD*Depth + LAD*Treatment + Depth*Treatment	64.7	0.628
	Best Fit	*k* = LAD + Depth + LAD*Depth	23.4*	0.502
	Global	*k* = log(LAD) + Depth + Treatment + log(LAD)*Depth + log(LAD)*Treatment + Depth*Treatment	64.7	0.628
	Best Fit	*k* = log(LAD)	20.4*	0.405
$\boldsymbol{\theta_L}$	Global	θ_L = Depth + Treatment + Depth*Treatment	4177.4	0.104
	Best Fit	θ_L = Treatment	4176.9	N/A

Table 2.3. ANOVA results for variables measured using direct methods in best fit regression models. All significant effects ($p<0.05$) are denoted with an asterisk (*). Abbreviations: *k* = coefficient of light extinction; LAD = leaf area density.

Variable	Model	Parameters	DF	F	P	R^2
k	Best Fit	LAD	1	19.2708	>0.001*	0.502
		Depth	2	0.6072	0.55	
		LAD*Depth	2	8.3871	>0.001*	
	Best Fit	log(LAD)	1	27.93	>0.001*	0.405

Table 2.4. Summary of the AICc model selection for variables dealing with the relationship between direct and indirect measurements. An asterisk (*) denotes the selected best fit models and the comparisons between direct and indirect methods whose significance are further evaluated in Table 5. Abbreviations: LAI = leaf area index; LAI_e = leaf area index measured with a ceptometer; LAD = Leaf area density; LAD_{cept} = leaf area density measured with a ceptometer; *k* coefficient of light extinction; k_{cept} = coefficient of light extinction measured with a ceptometer; LA = leaf area of ramet; LA_{3D} = leaf area of ramet measured with a 3D handheld scanner.

Variable	Model	Model Parameters	AICc	R^2
LAI	Global	$LAI = LAI_e + Treatment + LAI_e*Treatment$	185.9	0.884
	Best Fit	$LAI = LAI_e + Treatment + LAI_e*Treatment$	185.9*	0.884
	Comparison	$LAI = LAI_e$	193.8*	0.845
LAD	Global	$LAD = LAD_{cept} + Treatment + LAD_{cept}*Treatment$	182.6	0.631
	Best Fit	$LAD = LAD_{cept} + Treatment$	179.1*	0.613
	Comparison	$LAD = LAD_{cept}$	212.6*	0.519
k	Global	$k = k_{cept} + Treatment + k_{cept}*Treatment$	41.4	0.242
	Best Fit	$k = k_{cept} + Treatment$	38.0	0.204
	Global	$k = k_{cept} + Depth + k_{cept}*Depth$	43.1	0.213
	Best Fit	$k = Depth$	37.4	N/A
	Comparison	$k = k_{cept}$	40.0*	0.062
3D Scanner LA	Comparison	$LA = LA_{3D}$	N/A*	0.861

Table 2.5. ANOVA results for best fit regression models and models of individual comparisons dealing with the relationship between direct and indirect methods. All significant effects ($p<0.05$) are denoted with an asterisk (*). Abbreviations: LAI = leaf area index; LAI_e = leaf area index measured with a ceptometer; LAD = Leaf area density; LAD_{cept} = leaf area density measured with a ceptometer; *k* coefficient of light extinction; k_{cept} = coefficient of light extinction measured with a ceptometer; LA = leaf area of ramet; LA_{3D} = leaf area of ramet measured with a 3D handheld scanner.

Variable	Model Comparison	Parameters	DF	F	P	R^2	Slope
LAI	Comparison	LAI_e	1	316.25	>0.001*	0.845	0.9452
	Best Fit	LAI_e	1	394.6935	>0.001*		Browsed = 0.614
		Treatment	2	3.7379	0.03017*	0.884	Control = 0.855
		LAI_{cept}*Treatment	2	5.4548	0.00696*		Grazed = 1.112
LAD	Comparison	LAD_{cept}	1	44.184	>0.001*	0.519	0.6878
	Best Fit	LAD_{cept}	1	52.2721	>0.001*	0.613	0.5835
		Treatment	2	4.7529	0.01422*		
k	Comparison	k_{cept}	1	2.702	0.1079	0.062	0.2260
	Best Fit	k_{cept}	1	4.489	0.04037*	0.449	0.2356
		Treatment	1	28.116	>0.001*		
LA	Comparison	LA_{3D}	1	216.36	>0.001*	0.861	1.31091

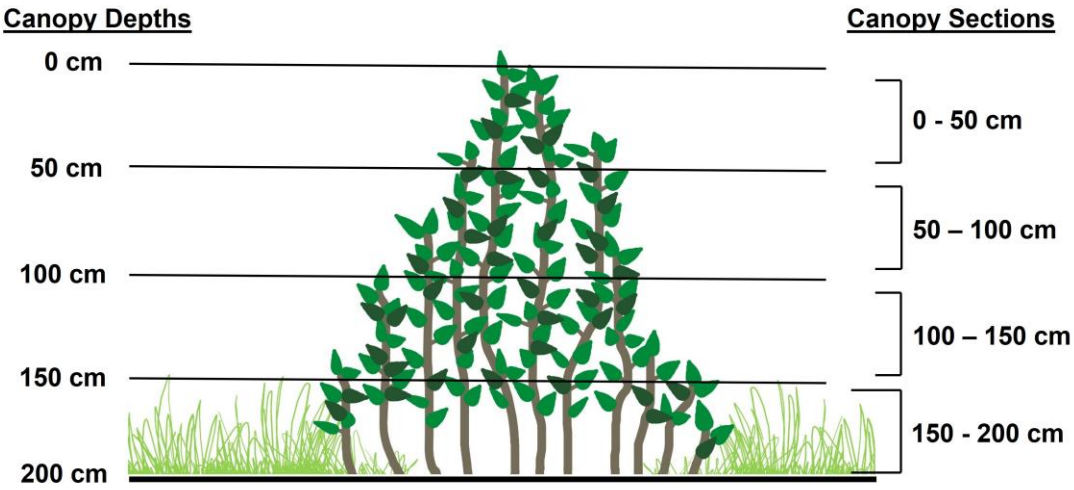

Figure 2.1. Schematic illustrating the canopy depths (0, 50, 100, 150 cm), and canopy sections (0-50, 50-100, 100-150, 150-200 cm) used in the study. The 200 cm depth and 150-200 cm section were only used to account for a small number of leaves in estimates of total LAI with direct methods and were excluded from all comparisons with indirect methods.

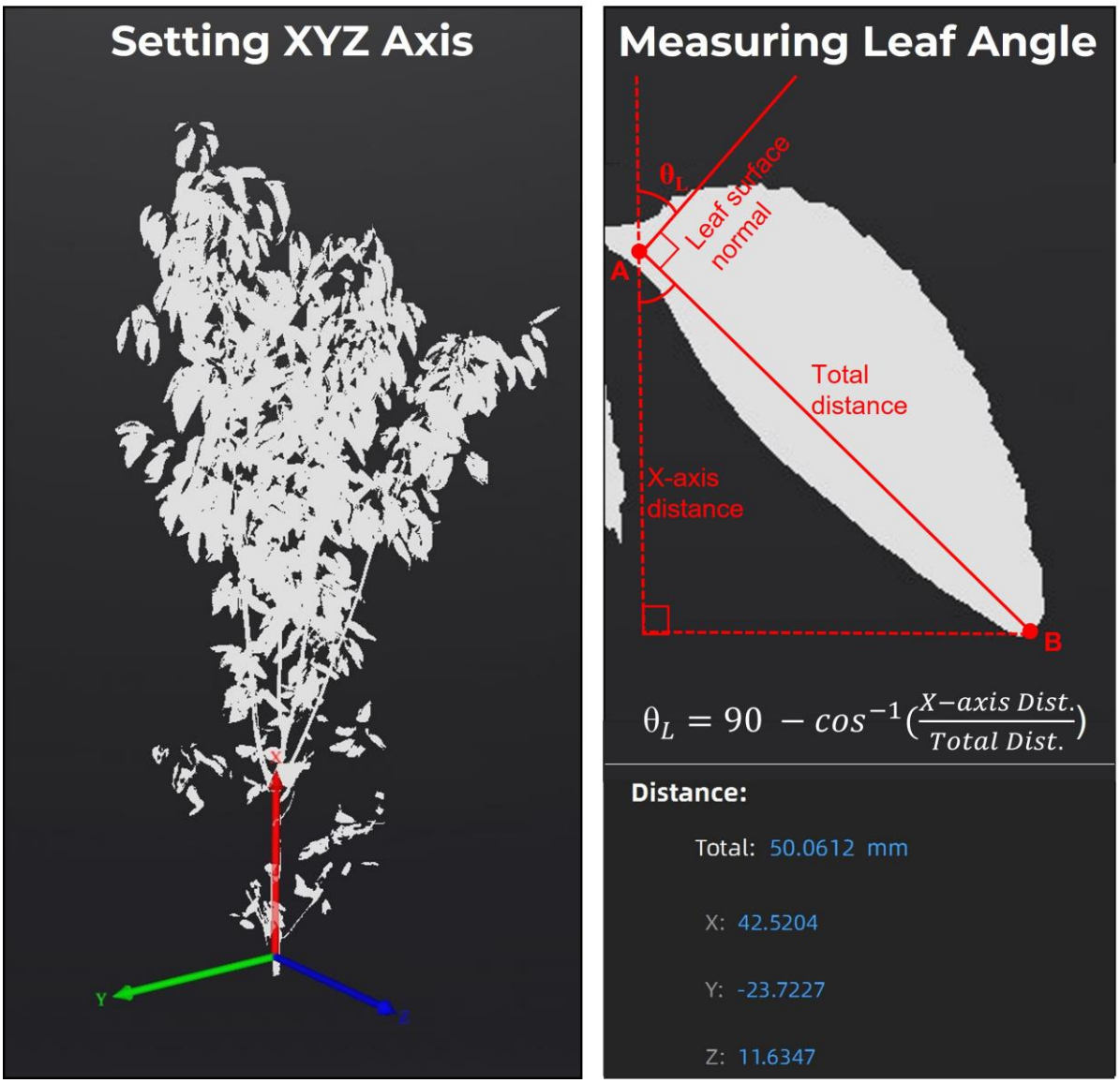

Figure 2.2. Image illustrating the measurement of leaf inclination angle (θ_L). Panel (A) illustrates the first step of the process. Cartesian coordinates are defined for the scanned ramet, with the X-axis (red) representing the zenith. Panel (B) illustrates the θ_L measurement for an individual leaf. θ_L was derived from the total distance between point A and point B and the vertical distance (x-axis/zenith) between point A and point B.

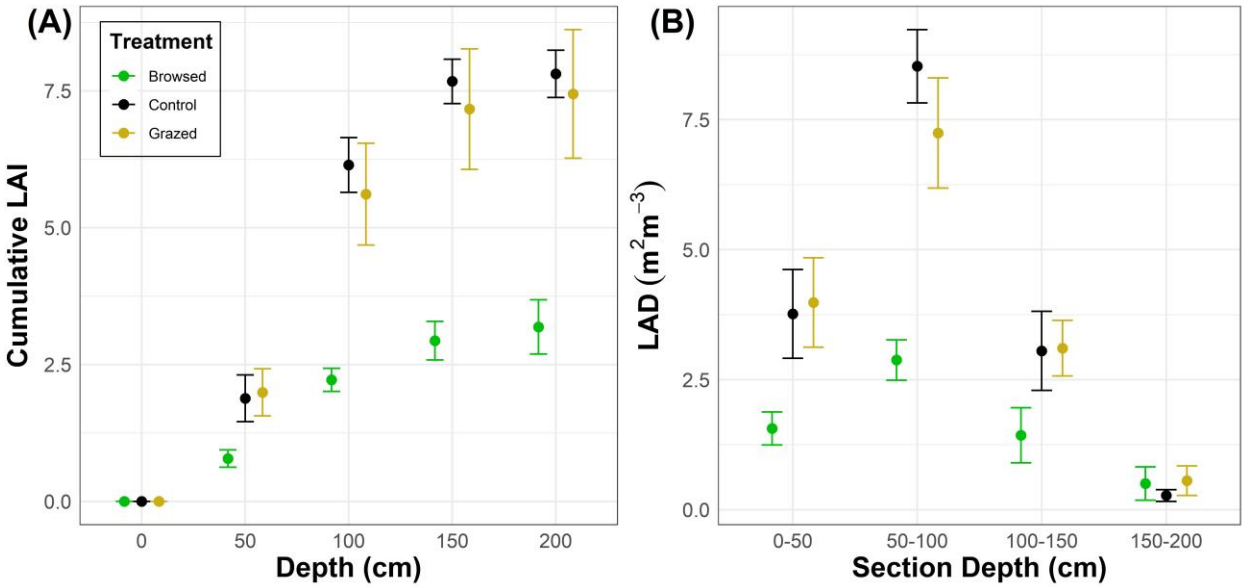

Figure 2.3. (A) Cumulative LAI measured by canopy depth and (B) LAD of individual canopy sections measured with direct methods in *C. drummondii* canopies varying in herbivory treatments (browsed, control, grazed). Point and whiskers represent the mean ± standard error.

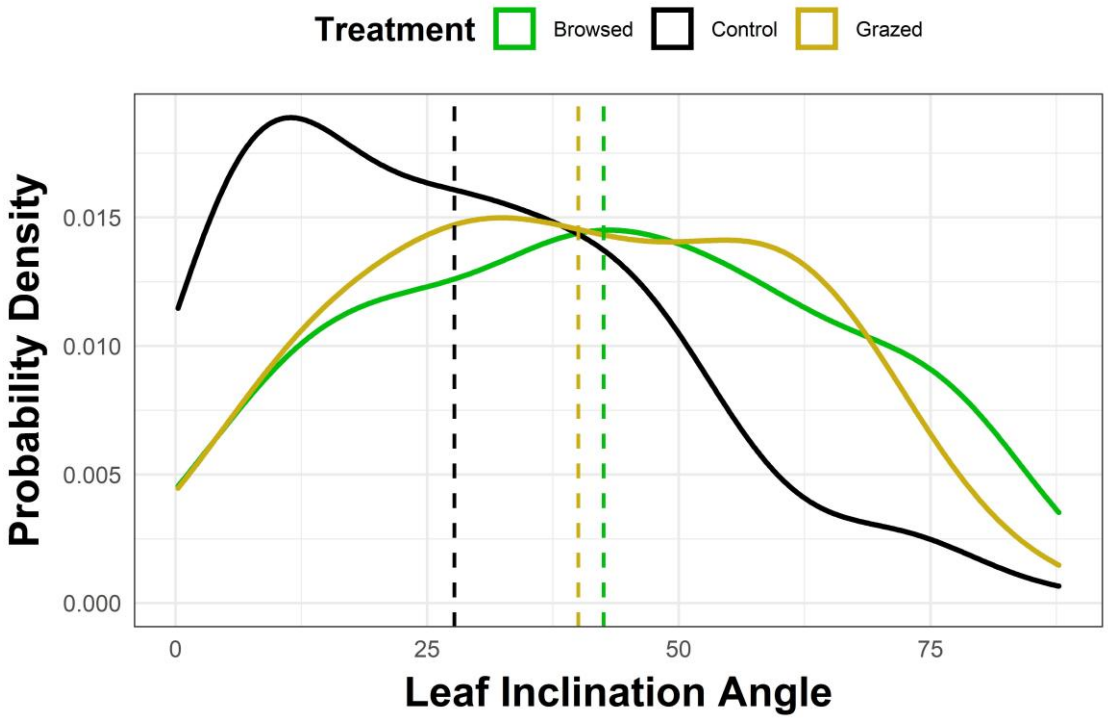

Figure 2.4. Density plot of the distribution of leaf inclination angles (θ_L) for leaves in canopies of *C. drummondii* varying by treatment. The dotted line denotes the mean θ_L for the specified treatment.

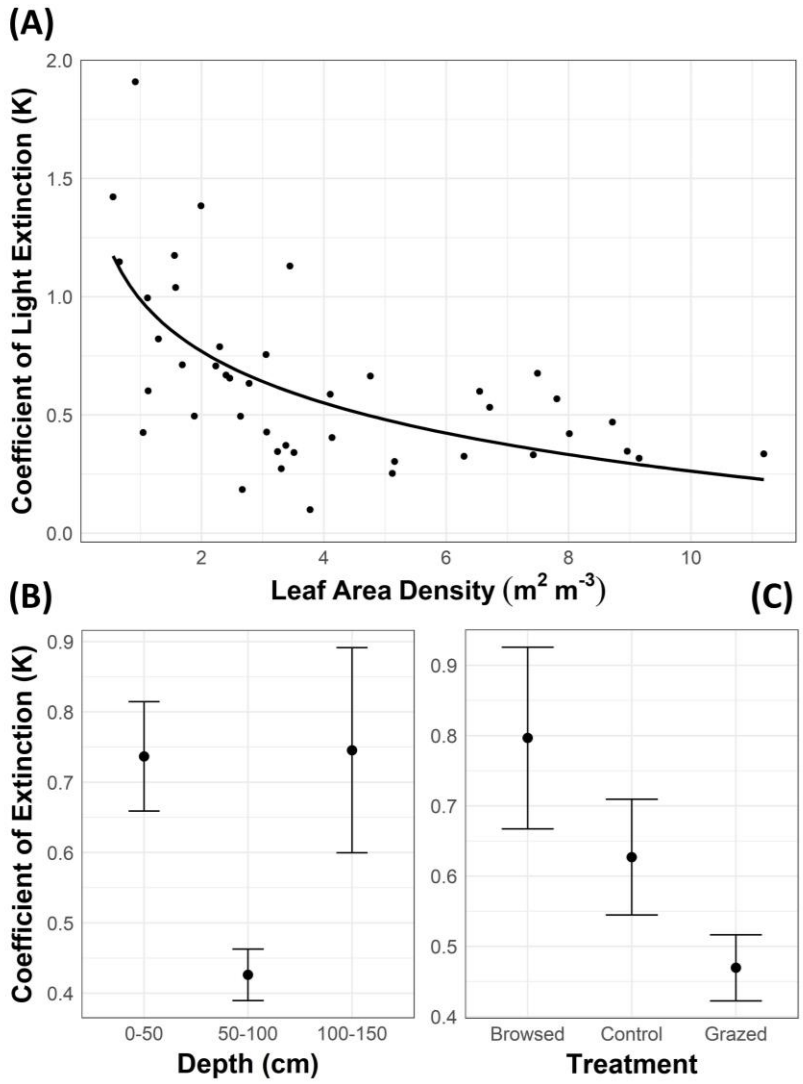

Figure 2.5. The coefficient of light extinction (*k*) from individual canopy sections varying by (A) Leaf area density, (B) depth, and (C) treatment. Point and whiskers represent the mean ± standard error of measurements.

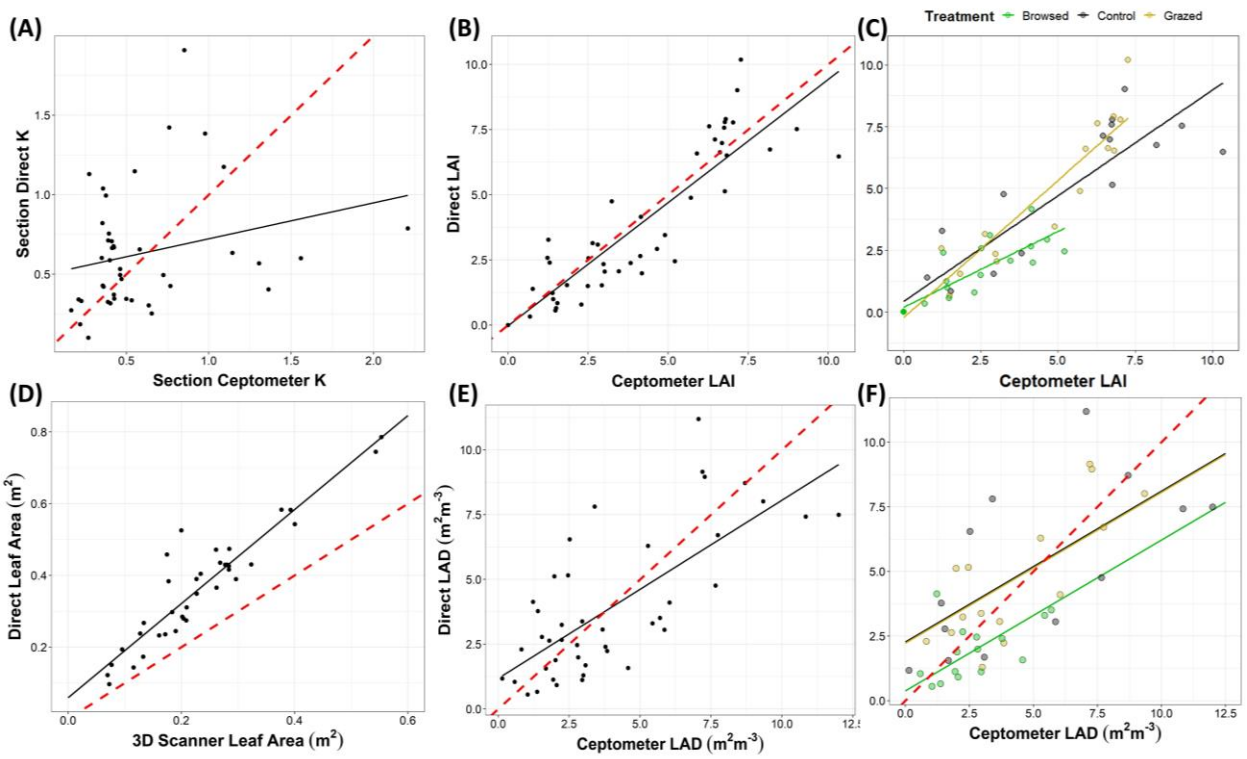

Figure 2.6. Linear regression models of the relationships between direct and indirect measurements of the variables (A) the coefficient of light extinction, (B) cumulative LAI, (C) cumulative LAI varying by depth, (D) ramet leaf area (3D scanner), (E) LAD of canopy sections (F) LAD of canopy sections varying by treatment. The dotted red line in plots A, B, D, and E denotes a 1:1 ratio between the direct and indirect method.

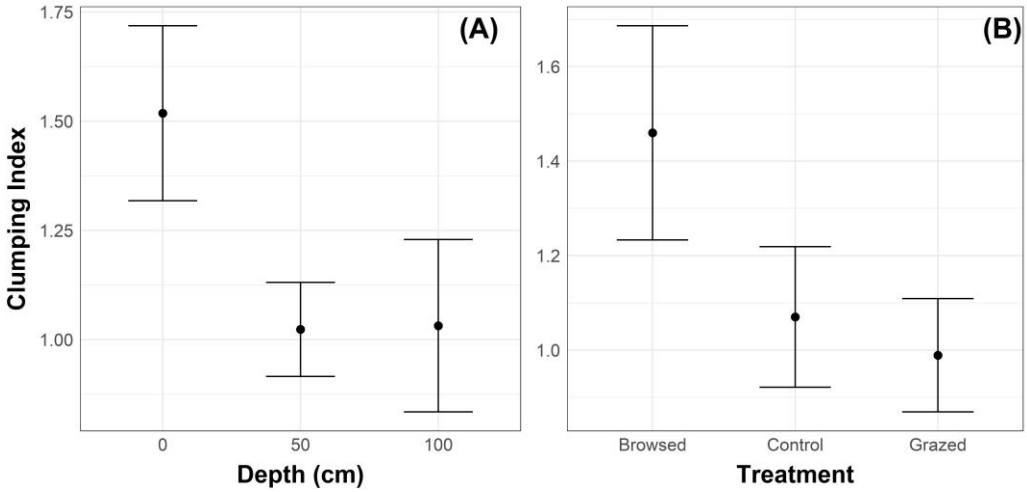

Figure 2.7. (A) The clumping index for individual canopy sections varying by depth, and (B) the clumping index for entire canopies of *C. drummondii* varying by treatment.

Chapter 3 - Intra-canopy leaf trait variation facilitates high leaf area index and compensatory growth in a clonal woody-encroaching shrub

Abstract

Leaf trait variation enables plants to take advantage of large gradients of light availability that exist across canopies of high leaf area index (LAI), allowing for greater net carbon gain while reducing light availability for understory competitors. While these canopy dynamics are well understood in forest ecosystems, studies of canopy structure of woody shrubs in grasslands are lacking, despite many species developing dense canopies with LAI values that exceed most temperate deciduous forests. To evaluate the investment strategy used by these shrubs, I investigated the vertical distribution of leaf traits and physiology across canopies of *Cornus drummondii*, the predominant woody encroaching shrub in the Kansas tallgrass prairie. I also examined the impact of disturbance by browsing and grazing on these factors. My results reveal that leaf mass per area (LMA) and leaf nitrogen per area (N_a) varied ~3-fold across canopies of *C. drummondii*, resulting in major differences in the physiological functioning of leaves. High LMA leaves had high photosynthetic capacity, while low LMA leaves used a novel strategy for maintaining light compensation points (LCP) below ambient light levels. *C. drummondii* also modified its vertical allocation of leaf traits in response to browsing, which increased light availability at deeper canopy depths. As a result, LMA and N_a increased at lower canopy depths, leading to a greater photosynthetic capacity deeper in browsed canopies compared to control canopies. This response, along with increased light availability, facilitated greater photosynthesis and resource-use efficiency deeper in browsed canopies compared to control canopies. My

results give a better understanding of how *C. drummondii* facilitates high LAI canopies and a compensatory growth response to browsing—both of which are key factors contributing to the success of *C. drummondii* and other species responsible for grassland woody encroachment.

Introduction

Over the past century, woody plants have expanded throughout grasslands worldwide in a phenomenon known as "woody plant encroachment" (Archer 1995, Stevens et al. 2017, Archer et al. 2017). In many cases, woody encroaching plants coexist with grasses, forming grass-tree mosaics, and have little impact on the structure and function of grasslands (Eldridge et al. 2011). In other cases, the dense canopies of some woody encroaching species can alter the light environment, resulting in a displacement of shade-intolerant grassland species and a gradual grassland-to-woodland transition (Ratajczak et al. 2012, Knapp et al. 2008, Brantley & Young 2007, Ratajczak et al. 2014). In mesic grasslands, many of the most abundant woody encroaching species have canopies with leaf area index (LAI) values exceeding that of many temperate deciduous forest communities (Brantley and Young 2007, Brantley and Young 2009). For example, *Cornus drummondii*, the predominant woody encroaching shrub in the tallgrass prairie of eastern Kansas (Ratajczak et al. 2011), and *Morella cerifera* in the coastal grasslands of Virginia, have mean LAI values of 8 and 10, respectively (**Figure 1A**; Knapp et al. 2008, Brantley & Young 2007). These values exceed the mean LAI of many temperate deciduous forests (~6.5; Norby et al. 2003, Asner et al. 2003), despite having canopies that are less than $1/10^{th}$ the height (1-5 m vs. >20 m for most temperate deciduous forests; Anderson et al. 2006, McGregor et al. 2020).

While a greater LAI increases total light capture and reduces light availability for shorter competitors, it also reduces light availability for successive leaf layers in the plant's own lower canopy (Monsi and Saeki 1953, Monsi and Saeki 2005).

Moreover, self-shading is greater when LAI is concentrated across a small vertical distance due to reduced penumbral effects on light penetration (Smith et al. 1989, Kramer et al. 2014, Van Pelt et al. 2016). As a result, short canopies experience greater self-shading and lower light availability compared to taller canopies (Smith et al. 1989, Van Pelt et al. 2016). Self-shading becomes detrimental to a plant when the cost of producing and maintaining more leaves (a greater LAI) outweighs the benefits of additional light capture (Saeki 1960, Reich et al. 2009). For this reason, an optimal LAI exists for maximizing canopy photosynthesis relative to the physiology of the plant (Saeki 1960, Hikosaka 2005, Waring 1983).

Gradients of light availability across canopies have cascading impacts on leaf-level physiology and whole plant carbon dynamics (Lambers 2008, Niinemets 2010). Woody shrubs and trees have evolved high intra-canopy variation in leaf morphology and physiology under varying light conditions to maximize light harvesting and net carbon fixation while avoiding over-excitation and damage to photosynthetic apparatuses (Long et al. 1994, Legner et al. 2014, Niinements 2007, 1998). Leaves in the upper canopy typically exhibit higher leaf mass per area (LMA) (Poorter et al. 2009, Ellsworth and Reich 1993) and more nitrogen per unit leaf area (N_a) compared to leaves in the lower canopy (Ellsworth and Reich 1993). Much of this nitrogen is allocated to RuBisCO (RuBP carboxylase-oxygenase), chlorophyll, and other photosynthetic proteins (Hikosaka and Terashima 1996, Evans 1989). Therefore, high LMA leaves typically contain greater amounts of RuBisCO per unit area, which facilitates greater maximum rates of carboxylation (Vc_{max}), as well as increased chlorophyll per unit area, which facilitates greater

maximum rates of electron transport (J_{max}) (Niinemets et al. 1998, Poorter and Evans 1998, Ripullone et al. 2003, Niinemets 2007, Carswell et al. 1999, Mendes et al. 2001). Together, J_{max} and Vc_{max} are rate-limiting steps to increasing maximum photosynthetic rates (A_{max}). (Powles 1984, Walker et al. 2014, Chen et al. 1993). These traits are beneficial in the upper canopy where photosynthetically active radiation (PAR) is high, but they are also associated with higher dark respiration rates (R_d) due to greater leaf energy demands (Ryan 1991, Amthor 2000, Bouma 2005, Givnish 1988).

Leaves in the lower canopy have lower LMA and N_a, resulting in decreased maximum photosynthetic rates and lower R_d rates (Poorter et al. 2009, Niinemets 2007, Ripullone et al. 2003, Ellsworth and Reich 1993). Leaves with lower R_d rates can reach the light compensation point (LCP) at lower PAR levels to achieve a net carbon gain from photosynthesis (Lewis et al. 2000, Walters et al. 1996, Moriwaki et al. 2019). LCP can also be minimized in shade leaves by allocating more nitrogen to thylakoids to increase apparent quantum yield (Φ) (Moriwaki et al. 2019), but this occurs at the expense of nitrogen allocation to RuBisCO which decreases the maximum carbon fixation rate of the leaf (Björkman 1981, Walters et al. 1996, Ögren and Evans 1993, Chen et al. 1993). Ecologically, species with a high capacity for intra-canopy variation in these traits can utilize leaves across a greater range of light conditions, maintain high LAI canopies, and maximize whole-canopy photosynthesis (Saeki 1960, Reich et al. 2009, Hikosaka et al. 2014, Niinemets et al. 2014, Chen et al. 1993).

The goal of my research was to determine the physiological mechanisms and traits that enable woody encroaching shrubs with dense canopies – specifically *Cornus drummondii* C.A. Mey. in tallgrass prairie – to utilize light efficiently while facilitating high LAI values across relatively short canopies. I examined the canopy structure, variation in leaf morphology and

physiology, and allocation of nutrients across a vertical canopy gradient of intact *C. drummondii* shrub islands (**Figure 3.1**) in areas grazed by bison, ungrazed, and in response to simulated browsing (to mimic elk herbivory, sensu O'Connor et al. 2020). While the vertical distribution of leaf traits and physiology is well understood within the canopies of tree species in forest ecosystems (Meir et al. 2002, Sack et al. 2006, Ninnemets 2007, Poorter et al. 2009, Legner et al. 2014, Mullin et al. 2009, Wyka et al. 2012, Rozendaal et al. 2006, Markesteijn et al. 2007), similar investigations have not been conducted within the canopies of woody encroaching shrubs in grasslands. Throughout canopies of *C. drummondii*, I hypothesized that: (1) high LAI values are facilitated by high variability in leaf morphology and physiology across a vertical canopy gradient, (2) variability in leaf morphology by canopy depth would lead to differences in physiological functioning that maximize net carbon gain of leaves, and (3) *C. drummondii* leaf morphology and physiology will vary in response to disturbance (browsing and grazing) and across the growing season.

Materials and Methods

Site Description

Research was conducted during the 2020 growing season (May-September) at the Konza Prairie Biological Station (KPBS), a 3,487-ha native tallgrass prairie in the northern Flint Hills ecoregion of Northeast Kansas, USA. The Flint Hills consists of the largest expanse of contiguous tallgrass prairie in North America. The region contains a heterogeneous landscape with varying topographic relief: shallow-soiled rocky uplands, steep slopes, and deep-soiled lowlands. KPBS is divided into experimental watersheds, each with a prescribed burn treatment (1, 2, 3, 4, or 20-year fire return intervals) and grazing treatment (bison, cattle, or no large

grazers). Historically, the plant community of KPBS was dominated by C_4 grasses, including *Andropogon gerardii*, *Sorghastrum nutans*, *Schizachyrium scoparium,* and *Panicum virgatum,* and was devoid of woody vegetation with the exception of riparian areas (Knapp et al. 1998). Today however, woody plants are abundant across all watersheds with a burn frequency of three years or more (Heisler et al. 2003, Ratajczak et al. 2014a). The most abundant woody encroaching plants include *Cornus drummondii*, *Juniperus virginiana, Rhus glabra, Prunus americana,* and *Gleditsia triacanthos* (Briggs et al. 2002, Nippert et al. 2021).

Study Design

At KPBS, I measured eco-physiological responses of the clonal woody shrub *Cornus drummondii* CA Mey (roughleaf dogwood). The growth form of *C. drummondii* consists of dense clonal patches of interconnected ramets termed "islands" (**Figure 3.1**). I utilized a stratified random sampling for 15 shrub islands of similar height and island circumference. I did not sample locations where clonal islands had grown together, blurring the boundaries between one individual and another. Only distinct islands with maximum heights greater than 1.5 meters were considered during sampling. Shrub islands were selected from the lowlands of two watersheds, N4D and K4A, approximately 2.4 km apart. Both watersheds are burned every four years and were last burned in the spring (March/April) of 2017. Watershed N4D is grazed by native bison, while watershed K4A does not contain any large mammalian grazers.

The experiment consisted of three treatments: grazed, simulated browsing, and control. For the grazed treatment, five islands were randomly selected on watershed N4D with heights ranging from 2.03 to 2.85 meters. In this treatment, bison have been grazing continuously year-round since 1992 and did so throughout the course of the study. Bison forage on grasses which make up a majority of their diet (~80-90%), along with forbs to a much lesser extent (~10-15%;

Plumb and Dodd 1993, Hecker et al. 2021, Raynor et al. 2016). Bison do consume some browse items (~5%), but these species are usually less than one meter in height and occur infrequently (Plumb and Dodd 1993). Bison do not typically consume a significant amount of leaves or stems of large woody trees and shrubs like *C. drummondii* (Knapp et al. 1999, Plumb and Dodd 1993, Coppedge et al. 1998, Raynor et al. 2016). However, grazing by bison has indirect impacts on woody plant distributions. Grass consumption by bison removes fine-fuels, leading to less intense fires and greater abundance of *C. drummondii* and other woody plants on grazed watersheds compared to ungrazed watersheds (Ratajczak et al. 2014, Briggs et al. 2002).

For the control and browsed treatments, ten islands were randomly selected on watershed K4A. Five islands were assigned to the control treatment, with no form of herbivory imposed, ranging from 2.02 to 2.45 m in height; and five islands were assigned to the browsed treatment ranging from 1.83 to 2.47 m in height. Simulated browsing was conducted on islands in the browsed treatment once during the early growing season (May 27th - June 1st), just before the start of sampling, and once during the mid-growing season (July 10th), nine days after my second sampling period. Fifty percent of an island's leaves were removed by hand by pulling from stems following the protocol of O'Connor et al. (2020). Significant amounts of new, non-woody stems were also removed during simulated browsing. This process was done as evenly as possible throughout the canopy on every ramet in the island above 10 cm from ground level. After removal, the leaves were deposited outside the study area.

Leaf Area Index

Leaf area index (LAI) was measured indirectly using an AccuPAR LP-80 ceptometer between the times of 12:00 and 15:00 in full sunlight in early July. The AccuPAR LP-80 ceptometer estimates LAI based on light transmission through the canopy (Bréda 2003). LAI measurements were made near the center of each shrub island across a vertical canopy gradient

consisting of four depths: 0 cm (top of the canopy), 50 cm, 100 cm, and 150 cm depth from the top of the canopy (**Figure 3.1b**). For each LAI measurement, eight instantaneous measurements of PAR were taken and averaged directly outside the canopy facing four directions, and eight instantaneous measurements of PAR were taken above a square meter area near the center of the shrub island at a given canopy depth facing four directions (two measurements per direction; 90-degree rotation between directions). LAI was calculated by the ceptometer from the averaged measurements.

Leaf-level Physiology

Leaf gas exchange was measured using a LI-6400XT open gas exchange system (LI-COR, Lincoln, Nebraska, USA). Instantaneous measures of net photosynthesis at ambient light intensity (A_{net}), stomatal conductance (g_s), and intrinsic water-use efficiency (iWUE; A_{net}/g_s) were measured at five positions within the canopy of each island of *C. drummondii* (see **Table 3.1** for a list of traits and their definitions). These positions consisted of a vertical canopy gradient in the center of the shrub island at four depths (**Figure 3.1b**): 0 cm (top of the canopy), 50 cm, 100 cm, and 150 cm depth from the top of the canopy. The fifth canopy position was on the outer perimeter ("out") of the island in full sunlight (**Figure 3.1b**). Ramets in the "out" position typically had leaves at similar heights to the surrounding grassy matrix. Instantaneous measurements were collected four times at regular intervals from early June to early September 2020. Measurements were taken from 9:00 to 15:00 on the newest, healthy, fully expanded leaves. At each canopy position, gas exchange was measured in situ for two leaves and averaged prior to further analysis. The reference chamber CO_2 concentration was set to 400 µmol CO_2 mol^{-1}, relative humidity was maintained between 40% and 60%, and the leaf chamber's PAR level was set to the ambient light level for each canopy position. An AccuPAR LP-80 ceptometer

was used to measure ambient PAR on a prior date with full sunlight. All PAR measurements were made within the same week as gas exchange measurements.

In addition to assessing instantaneous gas exchange, light response curves and *A*-c_i response curves were measured for all locations and canopy positions. Gas exchange measurements for both types of curves were made from July 3rd through July 17th. The light response curves were developed from in situ measurements at eight PAR intensities in the following order: 2000, 1200, 800, 400, 150, 50, 25, and 0 μmol m^{-2}-s^{-1}. For each of the light response curve measurements, the reference CO_2 level was set to 400 μmol CO_2 mol^{-1}, and the leaf was given a minimum of 90 seconds and a maximum of 450 seconds to equilibrate between changes in light intensity. Light response curves were used to calculate apparent quantum yield (Φ), LCP, R_d, and A_{2000}. Φ was calculated as the slope of a line through the points at PAR values of 0, 25, and 50 μmol m^{-2}-s^{-1}. LCP was calculated by fitting a line of best fit through the first few PAR intensities and then solving for LCP at a photosynthetic rate of 0 μmol m^{-2}-s^{-1}. R_d was calculated as the rate of photosynthesis at a PAR of 0 μmol m^{-2}-s^{-1}. Light saturated rates of photosynthesis (A_{sat}) could not be calculated because many of the leaves at depths 0 cm, 50 cm, and the "out" position did not asymptote. Therefore, A_{2000} was used as a proxy. A_{2000} was calculated as the rate of photosynthesis at 2000 μmol m^{-2}-s^{-1} of PAR and was equal to A_{sat} for most leaves at the 50 cm, 100 cm, and 150 cm depths.

Immediately following each light response curve, *A*-c_i response curves were collected by taking measurements at seven concentrations of CO_2 in the following order: 400, 250, 100, 50, 500, 800, and 1000 μmol CO_2 mol^{-1}. For all *A*-c_i curve measurements, the PAR intensity was set to 2000 μmol m^{-2} s^{-1}, and the leaf was given a minimum of 90 seconds and a maximum of 450 seconds to equilibrate between changes in [CO_2]. *A*-c_i response curves were developed using the

Farquhar-Berry-von Caemmerer model of photosynthesis (Farquhar et al. 1980, von Caemmerer and Farquhar 1981). This was done using the "fitaci" function from the "plantecophys" package (Duursma 2015) in R version 4.0.2 (R Core Team 2020). J_{max} and Vc_{max} were then derived from the curve using the "coef" function.

Leaf Traits

Following each gas exchange measurement, the measured leaf was immediately harvested. For leaf area, the petiole was removed, and area was measured on fresh leaves using a Li-3100 leaf area meter (Li-Cor, Lincoln, NE, USA). Leaves were then dried at 60 °C for a minimum of 72 hours, and leaf dry mass was measured thereafter. Leaf mass per area (LMA) was calculated by dividing leaf dry mass by leaf area (Pérez-Harguindeguy et al. 2013).

The leaf elemental abundance and stable isotopic signatures for carbon were performed at the Stable Isotope Mass Spectrometry Laboratory at Kansas State University. Dried leaves were ground using a Wig-L-Bug amalgamator, and samples were packed in tin capsules prior to analysis. Carbon and nitrogen stable isotope ratios as well as percent carbon and nitrogen of homogenized leaf samples were measured following combustion using an Elementar vario Pyro cube coupled to an Elementar Vision mass spectrometer for isotope analysis. Isotopic abundance ratios were converted to δ notation using the following equation:

$$\delta = [\frac{R_{sample}}{R_{standard}} - 1] * 1000$$

where R is the ratio of heavy to light isotopes for the sample and standard, respectively. Working laboratory standards were annually calibrated against the internationally accepted standard, Vienna Pee-Dee Belemnite for $\delta^{13}C$. Within-run and across-run variability of the laboratory working standard was < 0.05‰ for $\delta^{13}C$.

C:N ratio was calculated by dividing leaf percent carbon (%C) by leaf percent nitrogen (%N) for each sample. Relative photosynthetic nitrogen-use efficiency (PNUE) was calculated by dividing A_{net} by N_a. N_a was calculated using the following equation:

$$N_a = \frac{(\%N) \times (leaf\ mass)}{(leaf\ area)}$$

Data Analysis

To make comparisons among treatments, depths and sampling periods, repeated measures linear mixed-effects models were developed using the software package 'nlme' (Pinheiro et al. 2020) in R version 4.0.2 (R Core Team 2020). For each model, the response variable (PAR, LAI, LMA, N_{Area}, C:N, %N, A_{net}, $\delta^{13}C$, iWUE, and PNUE) were fit with canopy position, herbivory treatment (control, browsed, and grazed), and sampling date as fixed effects and replicate as a random effect. Linear mixed-effects models were also developed for the response variables extracted from *A*-c_i and light response curves (J_{max}, Vc_{max}, LCP, A_{2000}, Φ, and R_d). Parameters were fit with canopy position and herbivory treatment as fixed effects and replicate as a random effect. For all models, significant main effects and interactions are summarized in **Table 3.2.** For each significant interaction ($\alpha < 0.05$), a Tukey's HSD test was performed to make pairwise comparisons.

In addition to the mixed-effects models, all variables were arranged in a Pearson correlations matrix using the 'ggpairs' function from the package 'GGally' in R. One matrix was generated for leaves sampled throughout the growing season (**Figure A.3**) and another was made for the leaves sampled for the *A*-c_i and light response curves (**Figure A.4**).

Results

Light availability and LAI: For all treatments, PAR decreased and LAI increased significantly with canopy depth (**Table 3.2, Figure 3.2**). These trends were least pronounced for the browsed treatment where leaves where removed, resulting in lower LAI values and higher PAR levels in the canopy compared to the control and grazed treatments (**Figure 3.2**). In the control treatment, mean LAI of the canopy was 8.0 and PAR was reduced by 98% between the top (0 cm) and bottom (150 cm) of the canopy, whereas in the browsed treatment, mean LAI of the canopy was only 4.1 and PAR was reduced by 78% over the same vertical distance.

Leaf mass per area (LMA) and N per area (N_a): Both LMA and N_a varied significantly by treatment, depth, and across the growing season (**Table 3.2**). All two-way interactions were significant for LMA, as well as interactions for treatment*depth and date*depth for N_a. Overall, LMA and N_a decreased with depth for all treatments and at all time points during the growing season (**Figure 3.3**). LMA in upper canopy leaves (0 and 50 cm) and "out" position leaves increased throughout the growing season in all treatments (except the 50 cm depth in the control treatment; **Figure 3.3A**). LMA in lower canopy leaves in the control and grazed treatments remained relatively constant but increased throughout the growing season in the browsed treatment, resulting in greater LMA in lower canopy leaves in August and September compared to the control and grazed treatments (**Figure 3.3A**). Similarly, N_a in lower canopy leaves in the browsed treatment were higher in August and September compared to control and grazed treatments, but the differences were marginal (**Figure 3.3B; Table 3.2**).

Leaf stoichiometry: Overall, C:N increased significantly through the growing season (**Figure 3.4B, Table 3.2**). This increase was primarily driven by a decline in leaf %N (**Figure 3.4D, Table 3.2**). C:N also varied significantly by canopy depth, whereby values were greater in the "out" position compared to the 50, 100, and 150 cm depths (**Figure 3.4A, Table 3.2**). This response was primarily influenced by changes in %N by depth, which were greatest at the 50 and 100 cm depths and lowest in the 150 cm depth and "out" position (**Figure 3.4A, 4C, Table 3.2**). %N also varied by treatment with significantly greater values in the browsed treatment compared to the control and grazed treatments (**Figure A.1B**, **Table 3.2**).

A_{net}, PNUE, iWUE, and leaf $\delta^{13}C$: Instantaneous photosynthetic rates at ambient PAR (A_{net}) varied significantly by treatment, depth, date, and all two-way interactions (**Table 3.2**). Overall, photosynthetic rates were highest at the top of the canopy and on the outside of the island and decreased with canopy depth (**Figure 3.5a**). In the browsed treatment, photosynthetic rates in lower canopy leaves were significantly higher compared to the control and grazed treatments (**Figure 3.5a; Table 3.2**). Control and grazed treatments were similar at all depths until the last sampling period in September, where photosynthetic rates decreased in upper canopy leaves and outside of islands in the grazed treatment, resulting in smaller differences in photosynthetic rates between the top (0 cm) and bottom (150 cm) of the canopy compared to the control treatment (**Figure 3.5a**). Photosynthetic rates in the "out" position were similar to rates at the top (0 cm) of the canopy.

PNUE varied by all main effects and significant interactions between treatment*depth and date*depth (**Table 3.2**). PNUE declined with canopy depth in the control and grazed treatments throughout the first three sampling periods (June through August), but during the final

sampling period in September, PNUE was reduced in the upper canopy and "out" position resulting in smaller differences by depth (**Figure 3.5b**). In the browsed treatment, PNUE did not show the same declining trend with canopy depth—values stayed relatively constant through the canopy at all sampling dates (**Figure 3.5b**).

All main effects and interactions between treatment*date and treatment*depth varied significantly for iWUE (**Table 3.2**). Overall, iWUE values were highest during the last sampling period, and this trend was particularly pronounced in the grazed and control treatments (**Figure 3.5c**). A significant decline in iWUE by canopy depth was found in the control treatment during the July and September sampling periods, but otherwise iWUE stayed relatively constant throughout the canopy in the browsed and grazed treatments (**Figure 3.5c**).

Leaf $\delta^{13}C$ was lowest in the browsed treatment compared to the control and grazed treatments (**Figure A.1D**, **Table 3.2**). There was also a significant interaction between sampling date and canopy depth (**Table 3.2**). Leaf $\delta^{13}C$ was highest in the upper canopy and "out" position and declined with depth. At the 150 cm depth, Leaf $\delta^{13}C$ decreased throughout the growing season, leading to significantly greater values in the first sampling period compared to the final sampling period. ($p=0.027$; **Figure A.2**; **Table 3.2**).

***A*-c_i response curves:** J_{max} and Vc_{max}, derived from *A*-c_i response curves, varied significantly by canopy depth (**Table 3.3**). J_{max} and Vc_{max} were highest at the top of the canopy and declined with depth (**Table 3.4**), and both variables showed a nearly two-fold difference between the top (0 cm) and bottom (150 cm) of canopies. J_{max} and Vc_{max} in the "out" position were greater than the bottom of the canopy (100 and 150 cm depths), and had similar values to the top (0 and 50 cm depths) of the canopy (**Table 3.4**). J_{max} also varied significantly by treatment and Vc_{max} varied

marginally by treatment (p=0.055; **Table 3.3**), with greater values in browsed treatment canopies compared to the control and grazed treatments for both variables (**Table 3.3, Table 3.4**).

Light response curves: For all treatment types, both A_{2000} and Φ varied significantly by depth (**Table 3.3**). A_{2000} and Φ values were greatest to the top of the canopy (0 cm) and "out" position and decreased with depth in the canopy (**Table 3.4)**.

R_d and LCP both showed a significant treatment*depth interaction (**Table 3.3**). R_d and LCP declined with canopy depth in the control (marginally) and grazed treatments but stayed relatively constant throughout the canopy in the browsed treatment (**Table 3.4**). R_d and LCP in the "out" position were greater in the control treatment compared to the grazed treatment.

Pearson's correlation coefficients: For both LMA and N_a, significant positive correlations existed with the physiological parameters Φ, R_d, A_{2000}, J_{max}, and Vc_{max} (r= 0.62-0.87; **Figure A.3**). C:N ratio was not significantly correlated with any of the physiological parameters, and %N was only weakly correlated with Vc_{max} and J_{max}. Between physiological parameters, strong positive correlations existed between J_{max} and Vc_{max} (r=0.81), Vc_{max} and A_{2000} (r=0.91), and J_{max} and A_{2000} (r=0.73; **Figure A.3**). Φ was correlated with J_{max} (r = 0.74) and Vc_{max} (r= 0.60), but only weakly correlated with A_{2000}. For R_d, the strongest correlations occurred with J_{max} (r = 0.64) and Φ (r=0.72; **Figure A.3**).

From the seasonal measurements, PAR was strongly correlated with LMA (r=0.773) and N_a (r=0.790) of leaves as well as A_{net} (r=0.776) and $\delta^{13}C$ (r=0.728; **Figure A.4**), but PAR was not correlated with %N or C:N ratio of leaves. Within sampling periods, the morphological parameters LMA and N_a were strongly correlated to leaf A_{net} (r = 0.752 - 0.864), and $\delta^{13}C$ (r =

0.753 – 0821; **Figure A.4**). Between physiological parameters, correlations existed between A_{net} and $\delta^{13}C$, but both parameters were only weakly correlated to iWUE (**Figure A.4**).

Discussion

The mechanisms enabling *C. drummondii* and other woody encroaching shrubs with dense canopies to facilitate large light reductions across a small canopy distance is not well understood. This project investigated leaf morphological and physiological responses within discrete layers of *C. drummondii* canopies and the influence of simulated browsing (removing shrub leaves) and grazing (reducing competition from grasses) on these factors. Overall, my results indicated that: (1) Leaf morphology of *C. drummondii* varied greatly across a small vertical distance in response to light availability, resulting in major differences in the physiological functioning of leaves. High LMA leaves had high photosynthetic capacity, while low LMA leaves used a novel strategy for maintaining light compensation points (LCP) below ambient light levels. (2) *C. drummondii* leaf morphology and physiology were modified in response to disturbance by simulated browsing, but not grazing, within a single growing season, resulting in a compensatory growth response that facilitated greater photosynthetic capacity and resource-use efficiency in the lower-canopies of browsed *C. drummondii* islands.

Vertical variation in leaf morphology and resource allocation in *C. drummondii*.

Species with a high capacity to vary leaf morphology in response to light availability can utilize leaves across a greater range of light conditions to achieve greater LAI values. (Saeki 1960, Reich et al. 2009, Hikosaka et al. 2014, Niinemets et al. 2014, Chen et al. 1993). I found that *C. drummondii* canopies had LAI values greater than most temperate deciduous forests and reduced mean PAR by 97.5% despite having heights of only 1.5-3.0 m. Therefore, I

hypothesized that *C. drummondii* must be capable of high plasticity in leaf morphology and physiology. Supporting this hypothesis, I found that LMA and N_a varied ~3-fold across canopies of *C. drummondii*. Both parameters decreased with canopy depth and were strongly correlated with the ambient light conditions of the leaf. This is consistent with changes in LMA and N_a found across most forest canopies in response to light availability (Poorter et al. 2009). However, differences in LMA across a canopy are typically greater in tall species compared to shorter species (Cavaleri et al. 2010, Porter et al. 2009, Koch et al. 2004, Oldham et al. 2010) due to hydrostatic constraints on the canopy from increasing height (Niinemets 1997, Ishii et al. 2008). On average, LMA varies 4-fold across 100 m *Sequoia* canopies but only 2-fold across canopies of most tree species (Koch et al. 2004, Oldham et al. 2010, Sack et al. 2006, Poorter et al. 2009, Legner et al. 2014, Carswell et al. 1999, Gratani et al. 2006, Gratani et al. 2014, Rozendaal et al. 2006, Markesteijn et al. 2007, Wyka et al. 2012). While substantially shorter in stature, LMA varied more across *C. drummondii* canopies than the canopies of most tree species. Leaf C:N stayed constant across canopies despite the large variation in N_a indicating that changes in LMA resulted equally from changes in nitrogen and carbon. However, across the growing season, leaf C:N increased and %N decreased indicating that carbon accumulation contributed more to increases in LMA in upper canopy leaves across the growing season. This is likely due to thickening and enhanced lignification of cell walls in response to increased water limitation, and possibly the result of increased storage of starch and other non-structural carbohydrates—a product of high photosynthetic rates (Niinemets 1997, Edwards et al. 2010, Poorter et al. 2009, Moore et al. 1998, Paul and Foyer 2001). Overall, the high capacity of *C. drummondii* to vary leaf morphology, both across canopies and throughout the growing season, enables it to allocate

nitrogen and carbon advantageously in response to the large intra-canopy gradients of light found within high LAI canopies.

Influence of leaf morphology on leaf physiology and plant performance.

Variation in leaf morphology led to substantial differences in physiological functioning throughout the canopy that maximized leaf photosynthesis. Most physiological parameters were strongly correlated to leaf LMA and N_a (**Figure A.3, Figure A.4**). Photosynthetic parameters J_{max} and Vc_{max} were highest at the top of the canopy, leading to a greater A_{2000} compared to lower canopy leaves. This is beneficial at the top of the canopy where light availability is high. To maximize carbon gain under low-light conditions, LCP was reduced in lower canopy leaves relative to upper canopy leaves. This is critical to maintaining a high LAI since leaves that do not receive the minimum light required to reach photosynthetic compensation negatively impacts net canopy photosynthesis of the plant (Larcher 2003).

In theory, LCP decreases as a function of decreasing R_d and increasing Φ, but previous work suggests that Φ is relatively constant across canopies and that vertical variation in LCP is primarily driven by changes in R_d (Bond et al. 1999, Posada et al. 2009, Valladares et al. 1997, Avalos et al. 2007). Nonetheless, a few species such as *Pseudotsuga menziesii* var. glauca (Beissn.) Franco., *Abies grandis* (Dougl.) Lindl., and *Acer rubrum* L. have been found to have greater Φ in shade leaves compared to sun leaves, enabling shade leaves to further decrease LCP (Nippert and Marshall 2003, Kubiske and Pregitzer 1996, Oberbauer and Strain 1986, Langenheim et al. 1984). Decreased Φ may also result from increased leaf reflectance in upper canopy leaves to prevent damage to photosynthetic apparatus under high light conditions (Langenheim et al. 1984). Contrary to expectation, Φ in canopies of *C. drummondii* decreased with increasing canopy depth. A similar finding has been reported by Dusenge et al. (2015) in

tropical montane tree species with greater Φ in sun leaves compared to shade leaves, but this strategy has been rarely observed in other woody species. While decreased Φ negatively impacted the LCP of lower canopy leaves of *C. drummondii*, LCP was still maintained below ambient light levels, due to more than a 3-fold and 5-fold decrease in R_d in the control and grazed treatments. This may indicate a novel strategy for lowering LCP in *C. drummondii* canopies. Increasing Φ can require greater nutrient allocation to chloroplasts to increase the density of thylakoids, protein complexes, and concentrations of photosynthetic pigments (Moriwaki et al. 2019, Hikosaka and Terashima 1995). However, large reductions in R_d, enable *C. drummondii* to maintain LCP below ambient light conditions while theoretically allocating less nitrogen and nutrients to leaves compared to plants with a greater Φ (Moriwaki et al. 2019). While this strategy has benefits, a potential tradeoff exists. Lower canopy leaves of *C. drummondii* cannot utilize light efficiently in the presence of sunflecks compared to species with greater Φ values. However, sunflecks contribute less to carbon gain within canopies of species that concentrate LAI due to reduced penumbral effects (Smith et al. 1989, Stenberg et al. 1998, Van Pelt et al. 2016, Chazdon and Pearcy 1991). Brantley and Young (2009) found that sunflecks in mesic woody encroaching shrub canopies were smaller, shorter in duration, and less intense than those in deciduous forest canopies and contributed to only 5% of the total light below canopies compared to 32% below deciduous forest canopies. The scarcity of light from sunflecks in *C. drummondii* canopies may favor its strategy of reducing LCP, resulting in greater resource-use efficiency than otherwise possible.

Influence of browsing and grazing on *C. drummondii* canopy dynamics.

Previous research has shown that many species have a compensatory growth response that minimizes the impact of herbivory (Maschinski and Whitham 1989, McNaughton 1983).

O'Connor et al. (2020) found that ramet density of *C. drummondii* islands had not decreased after two consecutive years of high intensity browsing and maintained similar levels of nonstructural carbohydrates (glucose, sucrose, and starch) as un-browsed islands. These parameters did not decrease until fire and browsing were present in combination. In 2018 and 2019, Wedel et al. (2021) found that after four and five years of high intensity simulated browsing, *C. drummondii* islands still maintained similar recruitment and ramet mortality rates as un-browsed islands, and relative growth rates were similar between browsed and un-browsed islands during a droughted growing season in 2018. These results indicate that *C. drummondii* has a compensatory growth response to herbivory. However, the mechanisms behind this response are not well understood.

The results of this study provide a mechanistic explanation for the compensatory growth response of *C. drummondii*. Mechanisms leading to compensatory growth can be divided into intrinsic mechanisms involving changes in physiology and morphology/development, and extrinsic mechanisms involving modifications of the environment (McNaughton 1983). In *C. drummondii*, defoliation from browsing altered the canopy light environment, resulting in increased PAR values at deeper canopy depths compared to control islands. Over time, *C. drummondii* modified its leaf morphology and resource allocation throughout the canopy in response to browsing which resulted in greater LMA and N_a in lower canopies compared to the control treatment. This increase in LMA and N_a corresponded with the increase in light intensity at those depths. Leaves with increased LMA and N_a had a higher photosynthetic capacity due to increased J_{max}, Vc_{max}, and A_{2000}, and could reach greater photosynthetic rates at moderate light intensities (400-600) due to increased Φ. The resulting physiology in conjunction with higher PAR levels led to higher photosynthetic rates, increased iWUE, and increased PNUE in lower

canopy leaves of the browsed treatment compared to the control treatment and explains the compensatory growth response seen in *C. drummondii*. Improved iWUE may also explain why Wedel et al. (2021) found that browsed islands could maintain similar relative growth rates to un-browsed islands during a drought in 2018. The ability of *C. drummondii* to change its investment strategy within a single growing season is beneficial in grassland ecosystems where changes to the canopy light environment can occur as a result of frequent disturbance.

For the grazed treatment, I hypothesized that the distribution of LAI and leaf morphology of islands of *C. drummondii* in watersheds grazed by bison would differ from that in un-grazed (control) watersheds, and that these differences would lead to higher rates of whole canopy photosynthesis in the grazed treatment. Grazers such as cattle and bison do not directly consume *C. drummondii* or other woody shrubs, but previous work has shown that grazing by bison decreases grass abundance and reduces fire intensity, which facilitates positive feedbacks that drive the survival and spread of *C. drummondii* (Ratajczak et al. 2014, Briggs et al. 2002, Lett and Knapp 2003). However, my results indicate that grazing did not impact *C. drummondii* canopy dynamics. The distribution of LAI and PAR were similar to control canopies at all depths. Leaf morphology and physiology across canopies and in the "out" position of the grazed treatment also had very few differences from the control treatment. It is possible that the similarities between the control and grazed treatments are due to the absence of fire preceding sampling for this study, or it may also be that canopy dynamics are similar between the control and grazed treatments even when fire is present and increased abundance of *C. drummondii* in grazed watersheds results entirely from increased ramet survival in the presence of less intense fires. However, more research is needed to determine whether differences exist during years immediately following a fire.

Conclusions and Implications

Overall, my results have important implications for understanding the growth investment strategy of *C. drummondii* and other woody shrubs which enables them to achieve dense canopies, respond positively to periodic grassland disturbance, and ultimately facilitate successful encroachment in grassland ecosystems. This study revealed that these characteristics are driven by the capacity of *C. drummondii* to dramatically alter leaf traits in response to light gradients—both spatially to achieve dense canopies, and temporally to achieve compensatory growth.

Future research is needed to determine whether high intra-canopy variation in leaf traits exist in other woody encroaching species and whether this is a major characteristic differentiating woody encroaching species that cause large disruptions to grassland structure and function from those that coexist with grasses (Eldridge et al. 2011, Ratajczak et al. 2012). In *C. drummondii*, large leaf trait variation across canopies enables high-LAI values which lower light availability, displacing understory grasses, and resulting in fire suppression (Ratajczak et al. 2011, Lett and Knapp 2003). Once *C. drummondii* escapes fire it spreads rapidly across grasslands (Ratajczak et al. 2011). While leaf trait variation across a canopy is a major factor determining the optimal LAI to maximize whole-canopy photosynthesis (Saeki 1960, Hikosaka 2005), LAI is also limited by other factors such as water and nutrient availability (Asner et al. 2003). Future research is needed to determine the potential drivers of LAI in other woody encroaching shrubs and in other grasslands to better understand the extent to which intra-canopy variability in leaf traits (morphological and physiological) drives LAI of woody encroaching plants under different abiotic conditions. This relationship, along with a better understanding of canopy architectural traits, are central to determining why certain woody species become

dominant encroachers of grasslands, while most other woody species are either not encroaching or only minor encroachers.

References

Amthor JS (2000) The McCree de Wit-Penning de Vries-Thornley respiration paradigms: 30 years later. Annals of Botany 86:1–20.

Anderson J, Martin M, Dubayah ML, Dubayah R, Hofton M, Hyde P, Peterson B, Blair J, Knox R (2006) The use of waveform lidar to measure northern temperate mixed conifer and deciduous forest structure in New Hampshire Remote Sensing of Environment 105:248-261.

Archer SR (1995) Tree-grass dynamics in a thornscrub savanna parkland: reconstructing the past and predicting the future. Ecoscience 2:83-89.

Archer SR, Andersen EM, Predick KI, Schwinning S, Steidl RJ, Woods SR (2017) Woody plant encroachment: causes and consequences. In *Rangeland systems* (pp. 25-84). Springer, Cham.

Asner G, Scurlock J, Hicke J (2003) Global synthesis of leaf area index observations: implications for ecological and remote sensing studies. Global Ecology and Biogeography 122:191-205.

Avalos G, Mulkey SS, Kitajima K, Wright SJ. (2007) Colonization strategies of two liana species in a tropical dry forest canopy. Biotropica 39: 393–399.

Björkman, O (1981). Responses to Different Quantum Flux Densities. In *Physiological Plant Ecology I. Encyclopedia of Plant Physiology*. Springer, Berlin, Heidelberg.

Bouma T (2005) Understanding plant respiration: separating respiratory components versus a process-based approach. In *Plant respiration* (pp 177-194). Springer, Netherlands.

Brantley ST, Young DR (2007) Leaf-area index and light attenuation in rapidly expanding shrub thickets. Ecology 88:524–530.

Brantley ST, Young DR (2009) Contribution of sunflecks is minimal in expanding shrub thickets compared to temperate forest. Ecology 90:1021–1029.

Breda NJ (2003) Ground-based measurements of leaf area index: a review of methods, instruments and current controversies. Journal of Experimental Botany *54*:2403-2417.

Briggs JM, Knapp AK, Brock BL (2002) Expansion of woody plants in tall-grass prairie: A 15-year study of fire and fire-grazing interactions. American Midland Naturalist. 147:287–294.

Carswell FE, Meir P, Wandelli EV, Bonates LCM, Kruijt B, Barbosa EM, Nobre AD, Grace J, Jarvis PG (2000) Photosynthetic capacity in a central Amazonian rain forest. Tree Physiology 20:179–186.

Cavaleri MA, Oberbauer SF, Clark DB, Clark DA, Ryan MG (2010) Height is more important than light in determining leaf morphology in a tropical forest. Ecology 91:1730-1739.

Chen JL, Reynolds JF, Harley PC, Tenhunen JD (1993) Coordination theory of leaf nitrogen distribution in a canopy. Oecologia 93:63-69.

Coppedge BR, Leslie DM, Shaw JH (1998) Botanical composition of bison diets on tallgrass prairie in Oklahoma. Journal of Range Management 51:379–382.

Dusenge ME, Wallin G, Gårdesten J, Niyonzima F, Adolfsson L, Nsabimana D, Uddling J (2015) Photosynthetic capacity of tropical tree species in relation to leaf nutrients, successional group identity and growth temperature. Oecologia 177:1183–1194

Duursma RA (2015) Plantecophys - An R Package for Analysing and Modelling Leaf Gas Exchange Data. PLoS ONE 10(11): e0143346.

Edwards D, Jolliffe P, Ehret D (2010) Canopy profiles of starch and leaf mass per area in greenhouse tomato and the relationship with leaf area and fruit growth. Scientia Horticulturae 125:637–647.

Eldridge DJ, Bowker MA, Maestre FT, Roger E, Reynolds JR, Whitford WG (2011) Impacts of shrub encroachment on ecosystem structure and functioning: towards a global synthesis. Ecology Letters 14:709–722.

Ellsworth DS, Reich PB (1993) Canopy structure and vertical patterns of photosynthesis and related leaf traits in a deciduous forest. Oecologia 96:169-178.

Evans JR (1989) Partitioning of nitrogen between and within foliage grown under different irradiances. Australian Journal of Plant Physiology 16:533–548.

Farquhar GD, Von Caemmerer S, Berry JA (1980) A biochemical model of photosynthetic CO2 assimilation in leaves of C3 species. Planta 149:78-90.

Givnish TJ (1988) Adaptation to sun and shade: a whole-plant perspective. Australian Journal of Plant Physiology 15:63-92.

Gratani L, Covone F, Larcher W (2006) Leaf plasticity in response to light of three evergreen species of the Mediterranean maquis. Trees 20:549–558.

Gratani L (2014) Plant phenotypic plasticity in response to environmental factors. Advances in Botany 2014:1–17.

Hecker LJ, Coogan SCP, Nielsen SE, Edwards MA (2021) Latitudinal and seasonal plasticity in American bison (Bison bison) diets. Mammal Review 51:193–206.

Heisler JL, Briggs JM, Knapp AK. (2003) Long-term patterns of shrub expansion in a C4 - dominated grassland: Fire frequency and the dynamics of shrub cover and abundance. American Journal of Botany 90:423–428.

Hikosaka K, Terashima I (1996) Nitrogen partitioning among photosynthetic components and its consequence in sun and shade plants. Functional Ecology 10:335–343.

Hikosaka K. (2005) Leaf canopy as a dynamic system: ecophysiology and optimality in leaf turnover. Annals of Botany 95:521-53

Hikosaka K (2014) Optimal nitrogen distribution within a leaf canopy under direct and diffuse light. Plant, Cell & Environment 37:2077-2085.

Hikosaka K, Terashima I (1995) A model of the acclimation of photosynthesis in the leaves of C3 plants to sun and shade with respect to nitrogen use. Plant, Cell & Environment. 18:605-18.

Ishii HT, Jennings JM, Sillett SC, Koch GW (2008) Hydrostatic constraints on morphological exploitation of light in tall Sequoia sempervirens trees. Oecologia 156:751–763

Knapp AK, Briggs JM, Hartnett DC, Collins SC (1998) Grassland Dynamics: Long Term Ecological Research in Tallgrass Prairie. New York: Oxford University Press.

Knapp AK, Blair JM, Briggs JM, Collins SL, Hartnett DC, Johnson LC, Towne EG (1999) The keystone role of bison in North American tallgrass prairie. BioScience 49:39–50.

Knapp A, Briggs J, Collins S, Archer S, Bret-Harte M, Ewers B, Peters D, Young D, Shaver G, Pendall E (2008) Shrub encroachment in North American grasslands: Shifts in growth form dominance rapidly alters control of ecosystem carbon inputs. Global Change Biology 14:615–623.

Koch GW, Sillett SC, Jennings GM, Davis SD. 2004. The limits to tree height. Nature 428:851–854.

Kramer RD, Sillett SC, Carroll AL (2014) Structural development of redwood branches and its effects on wood growth. Tree Physiology 34:314 – 330.

Kubiske ME, Pregitzer KS (1996) Effects of elevated CO2 and light availability on the photosynthetic light response of trees of contrasting shade tolerance. Tree Physiology 16:351–358.

Lambers H, Chapin FS III, Pons TL (2008) Plant Physiological Ecology (2nd edition). Springer, New York.

Langenheim JH, Osmond CB, Brooks A, Ferrar PJ (1984) Photosynthetic responses to light in seedlings of selected Amazonian and Australian rainforest tree species. Oecologia 63:215-224.

Larcher W (2003) Physiological plant ecology. Springer, Berlin, Germany.

Legner N, Fleck S, Leuschner C (2014) Within-canopy variation in photosynthetic capacity, SLA and foliar N in temperate broad-leaved trees with contrasting shade tolerance. Trees 28:263–280.

Lett M, Knapp A (2003) Consequences of shrub expansion in mesic grassland: resource alterations and graminoid responses. Journal of Vegetation Science 14:487– 496.

Lewis JD, McKane RB, Tingey DT, Beedlow PA (2000) Vertical gradients in photosynthetic light response within an old growth Douglas-fir and western hemlock canopy. Tree Physiology 20:447–456.

Long SL, Humphries S, Falkowski PG. 1994. Photoinhibition of photosynthesis in nature. Annual Review of Plant Physiology and Plant Molecular Biology 45:633–62.

Markesteijn L, Poorter L, Bongers F (2007) Light-dependent leaf trait variation in 43 tropical dry forest tree species. American Journal of Botany 94:515–525.

Maschinski, J, Whitham TG. (1989) The continuum of plant responses to herbivory: the influence of plant association, nutrient availability, and timing. The American Naturalist 134:1-19.

McGregor IR, Helcoski R, Kunert N, Tepley AJ, Gonzalez-Akre EB, Herrmann V et al. (2020) Tree height and leaf drought tolerance traits shape growth responses across droughts in a temperate broadleaf forest. New Phytologist 231:601–616.

McNaughton SJ (1983) Compensatory plant growth as a response to herbivory. Oikos 40:329–336.

Meir P, Kruijt B, Broadmeadow M, Barbosa E, Kull O, Carswell F, Nobre A, Jarvis PG (2002) Acclimation of photosynthetic capacity to irradiance in tree canopies in relation to leaf nitrogen concentration and leaf mass per unit area. Plant, Cell & Environment 25:343–357.

Mendes MM, Gazarini LC, Rodrigues ML (2001) Acclimation of Myrtus communis to contrasting Mediterranean light environments–effects on structure and chemical composition of foliage and plant water relations. Environmental and Experimental Botany 45:165–178.

Monsi M, Saeki T (1953) Uber den Lichtfaktor in den Pflanzengesellschaften undseine Bedeutung fu¨r die Stoffproduktion. Japanese Journal of Botany 14:22–52.

Monsi M, Saeki T (2005) On the factor light in plant communities and its importance for matter production. Annals of Botany 95: 549–567.

Moore BD, Cheng SH, Rice J, Seemann JR (1998). Sucrose cycling, Rubisco expression, and prediction of photosynthetic acclimation to elevated atmospheric CO2. Plant, Cell & Environment 21:905-915.

Moriwaki T, Falcioni R, Tanaka FAO, Cardoso KAK, Souza LA, Benedito E, Nanni MR, Bonato CM, Antunes WC (2019) Nitrogen-improved photosynthesis quantum yield is driven by increased thylakoid density, enhancing green light absorption. Plant Science 278:1–11.

Mullin LP, Sillett SC, Koch GW, Tu KP, Antoine ME (2009) Physiological consequences of height-related morphological variation in Sequoia sempervirens foliage. Tree Physiology 29:999–1010.

Niinemets Ü (1997) Energy requirement for foliage construction depends on tree size in young Picea abies trees. Trees 11:420–431

Niinemets Ü, Kull O, Tenhunen JD (1998) An analysis of light effects on foliar morphology, physiology and light interception in temperate deciduous woody species of contrasting shade tolerance. Tree Physiology 18:681–696.

Niinemets Ü (2007) Photosynthesis and resource distribution through plant canopies. Plant, Cell and Environment 30:1052-1071.

Niinemets Ü (2010) A review of light interception in plant stands from leaf to canopy in different plant functional types and in species with varying shade tolerance. Ecological Research 25:693–714.

Niinemets Ü, Keenan TF, Hallik L (2014) A worldwide analysis of within-canopy variations in leaf structural, chemical and physiological traits across plant functional types. New Phytologist 205:973–993.

Nippert JB, Marshall JD (2003) Sources of variation in ecophysiological parameters in Douglas-fir and grand fir canopies. Tree Physiology 23:591-601.

Nippert JB, Telleria L, Blackmore P, Taylor JH, O'Connor RC (2021) Is a Prescribed Fire Sufficient to Slow the Spread of Woody Plants in an Infrequently Burned Grassland? A Case Study in Tallgrass Prairie. Rangeland Ecology & Management 78:79-89.

Norby RJ, Sholtis JD, Gunderson CA, Jawdy SS (2003) Leaf dynamics of a deciduous forest canopy: no response to elevated CO2. Oecologia 136:574-584.

Oberbauer SF, Strain BR (1986) Effects of canopy position and irradiance on the leaf physiology and morphology of Pentac- lethra macroloba (Mimosaceae). American Journal of Botany 73:409-416.

O'Connor RC, Taylor JH, Nippert JB (2020) Browsing and fire decreases dominance of a resprouting shrub in woody encroached grassland. Ecology 101:e02935.

Ögren E, Evans JR (1993) Photosynthetic light response curves. 1. The influence of CO2 partial pressure and leaf inversion. Planta 189:182–190.

Oldham AR, Sillett SC, Tomescu AMF, Koch GW (2010) The hydrostatic gradient, not light availability, drives height-related variation in Sequoia sempervirens (Cupressaceae) leaf anatomy. American Journal of Bodany 97:1–12.

Paul MJ, Foyer CH (2001) Sink regulation of photosynthesis. Journal of Experimental Botany 52:1383–1400.

Pérez-Harguindeguy N, Díaz S, Garnier E et al. (2013) New handbook for standardised measurement of plant functional traits worldwide. Australian Journal of Botany 61:167–234.

Pinheiro J, Bates D, DebRoy S, Sarkar D, Team RC (2021) nlme: linear and nonlinear mixed effects models. https://CRAN.R-project.org/ package=nlme.

Plumb GE, Dodd JL (1993) Foraging ecology of bison and cattle on mixed prairie: implications for natural area management. Ecological Applications 3:631–643.

Poorter H, Niinemets U, Poorter L, Wright IJ, Villar R (2009) Causes and consequences of variation in leaf mass per area (LMA): a meta-analysis. New Phytologist 182:565–588.

Poorter H, Evans JR (1998) Photosynthetic nitrogen-use efficiency of species that differ inherently in specific area. Oecologia 116:26– 37.

Posada JM, Lechowicz MJ, Kitajima K (2009) Optimal photosynthetic use of light by tropical tree crowns achieved by adjustment of individual leaf angles and nitrogen content. Annals of Botany 103:795-805.

Powles SB (1984) Photoinhibition of photosynthesis induced by visible light. Annual Review of Plant Physiology 35:15–44.

R Core Team (2020). R: A language and environment for statistical computing. R Foundation for Statistical Computing, Vienna, Austria. URL: https://www.R-project.org/.

Ratajczak Z, Nippert JB, Hartman JC, Ocheltree TW (2011) Positive feedbacks amplify rates of woody encroachment in mesic tallgrass prairie. Ecosphere 2:1–14.

Ratajczak Z, Nippert JB, Collins SL (2012) Woody encroachment decreases diversity across North American grasslands and savannas. Ecology 93:697–703.

Ratajczak Z, Nippert JB, Ocheltree TW (2014) Abrupt transition of mesic grassland to shrubland: evidence for thresholds, alternative attractors, and regime shifts. Ecology 95:2633– 2645.

Ratajczak Z, Nippert JB, Briggs JM, Blair JM (2014a) Fire dynamics distinguish grasslands, shrublands and woodlands as alternative attractors in the Central Great Plains of North American Journal of Ecology 102:1374–1385

Raynor EJ, Joern A, Nippert JB, Briggs JM (2016) Foraging decisions underlying restricted space use: Effects of fire and forage maturation on large herbivore nutrient uptake. Ecology and Evolution 16:5843-53.

Reich PB, Falster DS, Ellsworth DS, Wright IJ, Westoby M, Oleksyn J, Lee TD (2009) Controls on declining carbon balance with leaf age among 10 woody species in Australian woodland: do leaves have zero daily net carbon balances when they die? New Phytologist 183:153–166.

Ripullone F, Grassi G, Lauteri M, Borghetti M (2003) Photosynthesis–nitrogen relationships: interpretation of different patterns between Pseudotsuga menziesii and Populus × euroamericana in a mini-stand experiment. Tree Physiology 23:137–144.

Rozendaal DMA, Hurtado VH, Poorter L (2006). Plasticity in leaf traits of 38 tropical tree species in response to light; relationships with light demand and adult stature. Functional Ecology 20:207–216.

Ryan MG (1991) Effects of climate change on plant respiration. Ecological Applications 1:157–167

Sack L, Melcher PJ, Liu WH, Middleton E, Pardee T (2006) How strong is intracanopy leaf plasticity in temperate deciduous trees? American Journal of Botany 93:829–839.

Saeki T (1960) Interrelationships between leaf amount, light distribution and total photosynthesis in a plant community. Botanical Magazine Tokyo 73:55–63.

Smith WK, Knapp AK, Reiners WA (1989) Penumbral effects on sunlight penetration in plant communities. Ecology 70:1603-1609.

Staver CA, WJ Bond, WD Stock, Van Rensburg SJ, Waldram MS (2009) Browsing and fire interact to suppress tree density in an African savanna. Ecological Applications 19:1909–1919.

Stenberg P (1998) Implications of shoot structure on the rate of photosynthesis at different levels in a coniferous canopy using a model incorporating grouping and penumbra. Functional Ecology 12:82–91.

Stevens N, Lehmann CER, Murphy BP, Durigan G (2017) Savanna woody encroachment is widespread across three continents. Global Change Biology 23:235–244.

Valladares F, Allen MT, Pearcy RW (1997) Photosynthetic response to dynamic light under field conditions in six tropical rainforest shrubs occurring along a light gradient. Oecologia 111:505–14.

Van Pelt R, Sillett SC, Kruse WA, Freund JA, Kramer RD (2016). Emergent crowns and light-use complementarity lead to global maximum biomass and leaf area in Sequoia sempervirens forests. Forest Ecology and Management 375:279–308.

Von Caemmerer S, Farquhar GD (1981) Some relationships between the biochemistry of photosynthesis and the gas exchange of leaves. Planta 153:376-387

Walker AP, Beckerman AP, Gu LH, Kattge J, Cernusak LA, Domingues TF, Scales JC, Wohlfahrt G, Wullschleger SD, Woodward FI (2014) The relationship of leaf photosynthetic traits - Vcmax and Jmax - to leaf nitrogen, leaf phosphorus, and specific leaf area: a meta-analysis and modeling study. Ecology and Evolution 4:3218–3235.

Walters M, Reich P (1996) Are shade tolerance, survival, and growth linked? Low light and nitrogen effects on hardwood seedlings. Ecology 77:841-853.

Waring RH (1983) Estimating forest growth and efficiency in relation to canopy leaf area. Advances in Ecological Research 13:327-354

Wedel E, Nippert JB, Hartnett D (2021) Fire and browsing interact to alter intra-clonal stem dynamics of an encroaching shrub in tallgrass prairie. Oecologia 196:1039–1048.

Wyka TP, Oleksyn J, Zytkowiak R, Karolewski P, Jagodzinski AM, Reich PB (2012) Responses of leaf structure and photosynthetic properties to intra-canopy light gradients: a common garden test with four broadleaf deciduous angiosperm and seven evergreen conifer tree species. Oecologia 170:11–24.

Tables and Figures

Table 3.1. List of measured canopy and leaf traits with a brief description and units accompanying each variable.

Canopy Structure & Light Environment	Units	Description
Leaf area index (LAI)	Unitless	Canopy leaf area per unit ground area
Photosynthetically active radiation (PAR)	μmol m^{-2} s^{-1}	Amount of light available for photosynthesis
Leaf Morphological Traits		
Leaf mass per area (LMA)	g m^{-2}	Mass of leaf tissue per leaf area
Leaf nitrogen per area (N_a)	g m^{-2}	Mass of leaf nitrogen per leaf area
Percent leaf nitrogen (%N)	%	Percentage of leaf composition that is nitrogen
C:N ratio	Unitless	The ratio of leaf carbon to leaf nitrogen
Leaf Physiological Traits		
Maximum rate of carboxylation (Vc_{max})	μmol m^{-2} s^{-1}	Maximum rate of carboxylation
Maximum rate of electron transport (J_{max})	μmol m^{-2} s^{-1}	Maximum rate of electron transport
Light compensation point (LCP)	μmol m^{-2} s^{-1}	PAR level required for photosynthesis to equal respiration
Dark respiration (R_d)	μmol m^{-2} s^{-1}	Leaf respiration rate at 0 μmol m^{-2} s^{-1} of PAR
Apparent quantum yield (Φ)	mol CO_2 (mol incident photon)$^{-1}$	CO_2 consumption per incident photon
Photosynthetic rate at 2000 μmol m^{-2} s^{-1} (A_{2000})	μmol m^{-2} s^{-1}	Photosynthetic rate at 2000 μmol m^{-2} s^{-1} of PAR
Leaf Integrative Traits		
Photosynthetic rate at ambient PAR (A_{net})	μmol m^{-2} s^{-1}	Photosynthetic rate at ambient PAR
Intrinsic water-use efficiency (iWUE)	(μmol m^{-2} s^{-1}) g_s^{-1}	photosynthesis divided by stomatal conductance
$\delta^{13}C$	Unitless	ratio of the rare to common stable isotopes (^{13}C:^{12}C) in the sample compared to a standard in permil (‰)
Photosynthetic nitrogen-use efficiency (PNUE)	μmol g^{-1} s^{-1}	photosynthesis per gram of nitrogen

Table 3.2. Summary of the mixed effects models analysis of variance. Table contains all variables that were measured at multiple periods throughout the growing season. All significant effects ($p<0.05$) are bold font and insignificant effects are normal font ($p>0.05$). Abbreviations: PAR = photosynthetically active radiation; LMA = leaf mass per area; N_a = leaf nitrogen per unit area; %N = percent leaf nitrogen; A_{net} = instantaneous photosynthetic rate at ambient light intensity; iWUE = intrinsic water-use efficiency; PNUE = photosynthetic nitrogen-use efficiency.

	Response Variable								
Predictor Variable	PAR	LMA	N_a	%N	C:N	A_{net}	iWUE	$\delta^{13}C$	PNUE
Date	0.5095	**<0.0001**	**0.0092**	**<0.0001**	**<0.0001**	**<0.0001**	**<0.0001**	**0.0038**	**<0.0001**
Treatment	**<0.0001**	**<0.0001**	**<0.0001**	**0.0029**	**0.0068**	**<0.0001**	**<0.0001**	**0.0005**	**<0.0001**
Depth	**<0.0001**	**<0.0001**	**<0.0001**	**0.0013**	**<0.0001**	**<0.0001**	**<0.0001**	**<0.0001**	**<0.0001**
Date*Treatment	0.0748	**<0.0001**	0.1264	0.1035	0.1897	**0.001**	**<0.0001**	0.8133	0.1179
Date*Depth	0.4579	**<0.0001**	**0.0135**	0.5434	0.4608	**0.0003**	0.4916	**0.0144**	**0.0054**
Treatment*Depth	**<0.0001**	**0.0001**	**0.0055**	0.4185	0.2331	**<0.0001**	**0.0011**	0.1844	**<0.0001**
Date*Treatment*Depth	0.5509	0.6784	0.1988	0.6456	0.5382	0.6342	0.7976	0.9293	0.592

Table 3.3. Summary for the mixed effects model analysis of variance. Table summarizes response variables that were only measured during one period of the growing season. All significant effects ($p<0.05$) are bold font and insignificant effects are normal font ($p>0.05$). An asterisk is placed next to effects with marginal differences. Abbreviations: Vc_{max} = maximum velocity of carboxylation; J_{max} = maximum velocity of electron transport; LCP = light compensation point; R_d = dark respiration; Φ = apparent quantum yield; A_{2000} = photosynthetic rate at 2000 μmol m^{-2}-s^{-1}; LAI = leaf area index.

Predictor Variable	Response Variable						
	LAI	Vc_{max}	J_{max}	LCP	R_d	Φ	A_{2000}
Treatment	**<0.0001**	*0.0553	**0.0138**	**0.0020**	**0.0079**	0.4870	0.1284
Depth	**<0.0001**	**<0.0001**	**<0.0001**	**0.0059**	**<.0001**	**<0.0001**	**<0.0001**
Treatment*Depth	**0.0001**	0.6123	0.6728	**0.0028**	**0.0041**	0.8169	0.4632

Table 3.4. Summary of means and standard errors for parameters extracted from the *A*-c_i and light response curves. See Table 1 for variable units. Abbreviations: Vc_{max} = maximum velocity of carboxylation; J_{max} = maximum velocity of electron transport; LCP = light compensation point; R_d = dark respiration; Φ = apparent quantum yield; A_{2000} = photosynthetic rate at 2000 μmol m^{-2}-s^{-1}.

		Vc_{max} (μmol m^{-2} s^{-1})		J_{max} (μmol m^{-2} s^{-1})		LCP (μmol m^{-2} s^{-1})		R_d (μmol m^{-2} s^{-1})		Φ (mol / mol)		A_{2000} (μmol m^{-2} s^{-1})	
Treatment	**Depth**	Mean	SE	Mean	SE	Mean	SE	Mean	SE	Mean	SE	Mean	SE
Control	Out	39.97	2.11	111.19	3.13	49.58	7.61	3.63	0.36	0.0860	0.0043	13.09	0.45
	0	41.39	5.35	120.16	13.60	41.76	5.69	3.64	0.64	0.0944	0.0118	9.81	2.23
	50	35.06	5.49	111.93	20.48	27.74	4.32	2.38	0.51	0.0885	0.0090	7.11	0.86
	100	18.50	2.13	67.63	2.71	17.60	7.32	1.22	0.45	0.0775	0.0020	5.86	0.26
	150	12.89	3.83	39.52	10.13	22.73	9.24	1.16	0.39	0.0565	0.0075	3.29	1.45
	All	28.30	3.02	87.68	8.66	32.14	3.71	2.46	0.31	0.0816	0.0044	7.89	0.90
Browsed	Out	38.94	5.41	105.29	8.34	29.38	3.56	2.29	0.34	0.0883	0.0100	9.93	1.89
	0	46.85	5.19	144.01	15.90	36.10	2.44	3.15	0.50	0.0967	0.0100	11.99	1.08
	50	36.67	4.56	114.80	13.35	30.46	4.40	2.60	0.40	0.0893	0.0071	9.60	0.32
	100	34.52	5.72	109.13	9.26	45.02	8.09	3.12	0.31	0.0861	0.0081	9.67	1.75
	150	20.46	4.19	78.13	10.40	37.90	9.23	2.16	0.56	0.0635	0.0038	5.06	0.55
	All	34.94	2.77	108.61	6.34	35.95	2.83	2.68	0.19	0.0851	0.0040	9.29	0.70
Grazed	Out	35.21	3.32	94.72	13.82	21.54	4.80	1.56	0.34	0.0776	0.0040	9.38	1.61
	0	40.33	3.90	126.32	24.11	42.20	6.45	3.94	0.67	0.1033	0.0066	9.59	0.79
	50	30.47	6.00	98.82	14.56	24.50	2.93	2.11	0.37	0.0897	0.0073	7.71	1.67
	100	22.31	3.77	66.38	7.37	13.70	2.95	0.96	0.25	0.0663	0.0046	6.65	1.39
	150	18.89	4.26	52.29	11.80	11.95	2.86	0.74	0.27	0.0545	0.0100	4.29	2.32
	All	29.44	2.40	87.71	8.21	23.23	2.86	1.91	0.29	0.0793	0.0044	7.66	0.75
All	Out	37.90	2.25	103.20	5.72	32.58	4.47	2.42	0.31	0.0835	0.0036	10.69	0.92
	0	42.66	2.63	129.87	10.78	40.30	3.01	3.61	0.34	0.0983	0.0053	10.36	0.88
	50	33.79	3.02	107.77	8.80	27.57	2.20	2.37	0.24	0.0892	0.0042	8.14	0.65
	100	25.11	2.87	82.00	6.88	26.00	5.23	1.81	0.32	0.0766	0.0039	7.50	0.87
	150	17.41	2.36	56.65	7.19	24.19	5.15	1.35	0.29	0.0582	0.0041	4.21	0.87

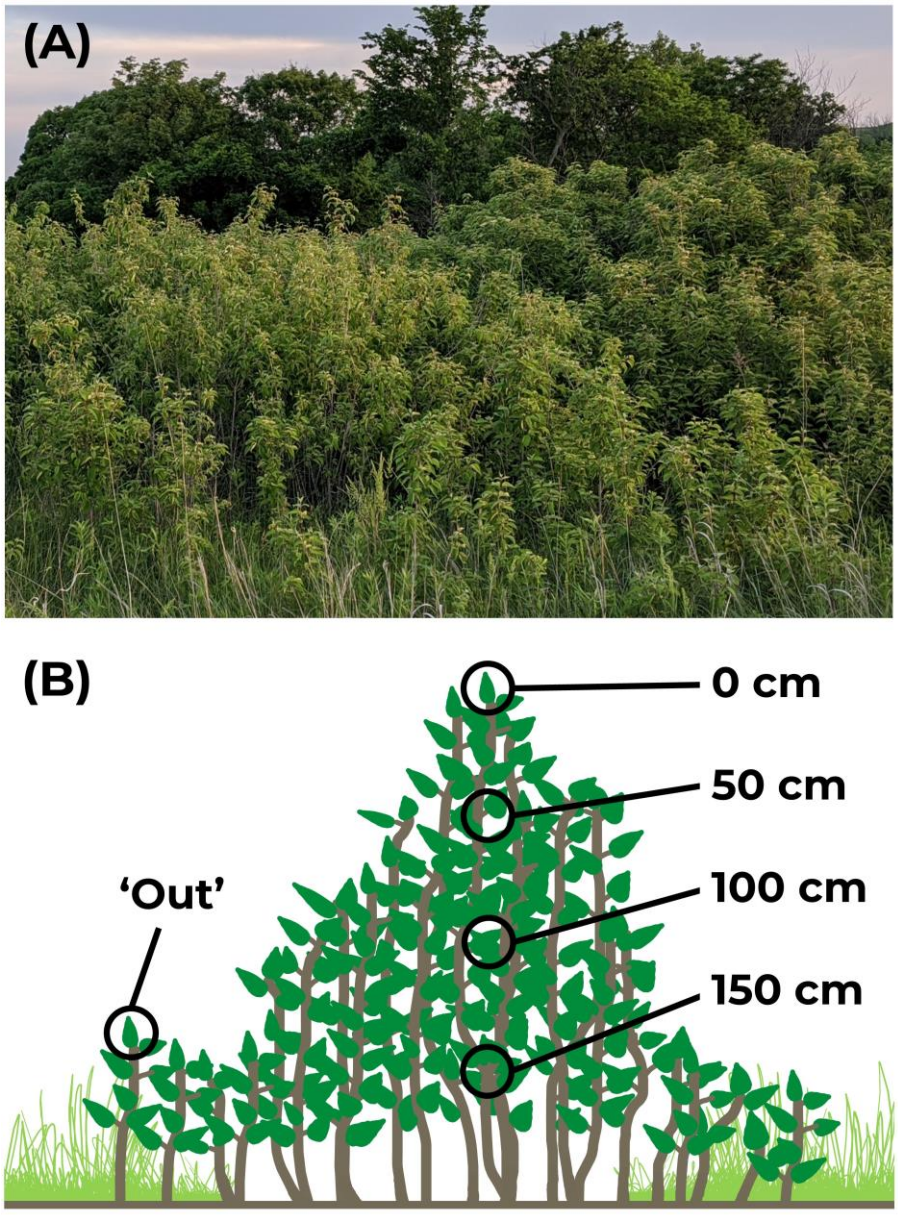

Figure 3.1. (A) A large island of *C. drummondii* with a dense canopy on watershed K4A at Konza Prairie Biological Station, Manhattan, Kansas. The growth form of *C. drummondii* consists of dense clonal patches of interconnected ramets termed "islands". (B) Diagram showing a cross section through the center of a *C. drummondii* island illustrating its growth form and my sampling locations. Black circles represent the measurement location for each canopy depth. Diagram credit: *C. drummondii* island animation by Emily Wedel. Photo by Rachel Keen.

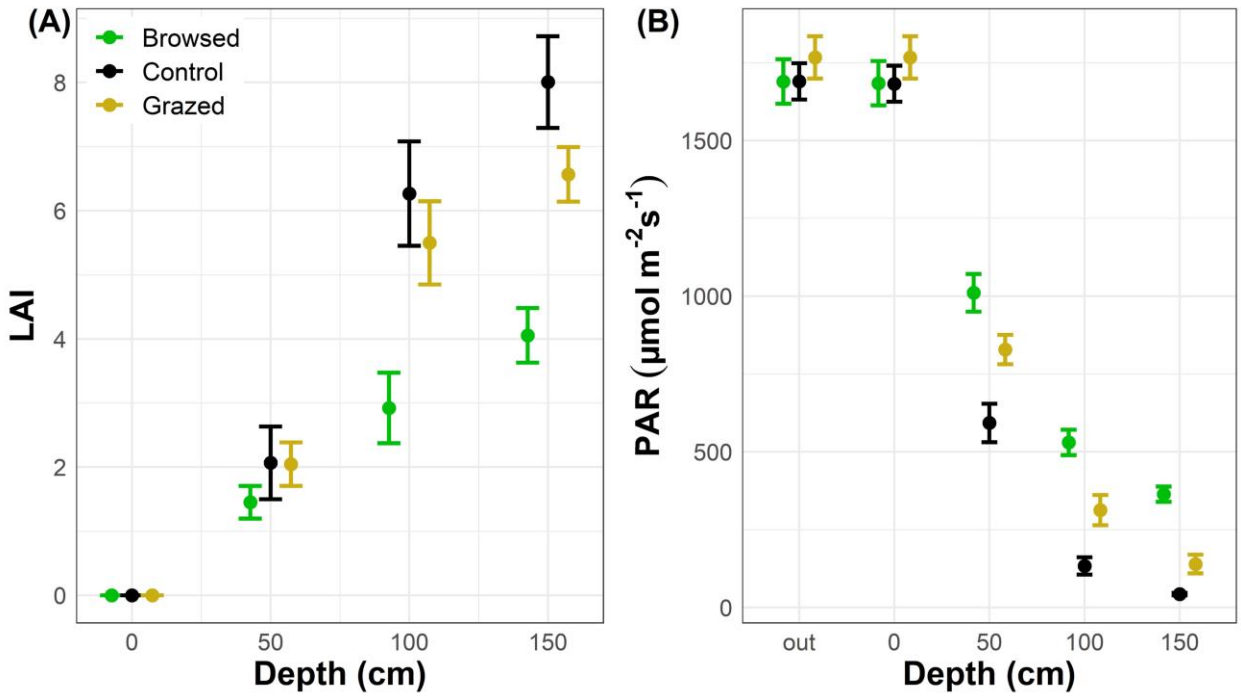

Figure 3.2. (A) LAI and (B) PAR measured in *C. drummondii* canopies at varying canopy depths (0 cm, 50 cm, 100 cm, and 150 cm) and herbivory treatments (browsed, control, grazed). Point and whiskers represent the mean ± standard error of the one sampling period for LAI, and the mean ± standard error for all four sampling periods for PAR.

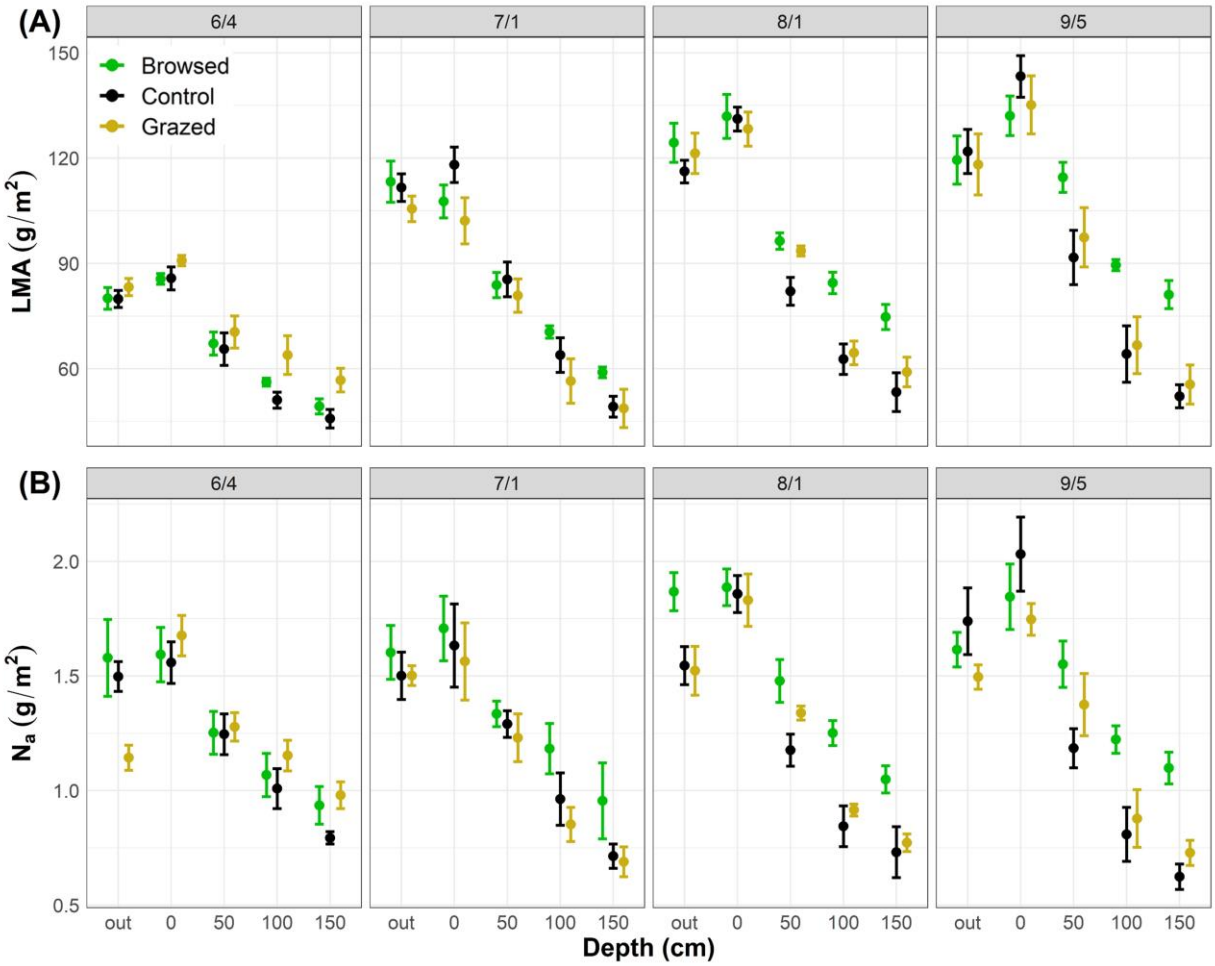

Figure 3.3. (A) LMA and (B) N_a of leaves in *C. drummondii* canopies varying by canopy position (out, 0 cm, 50 cm, 100 cm, and 150 cm), herbivory treatment (browsed, control, and grazed), and sampling period (6/4/, 7/1, 8/1, 9/5). Point and whiskers represent the mean ± standard error.

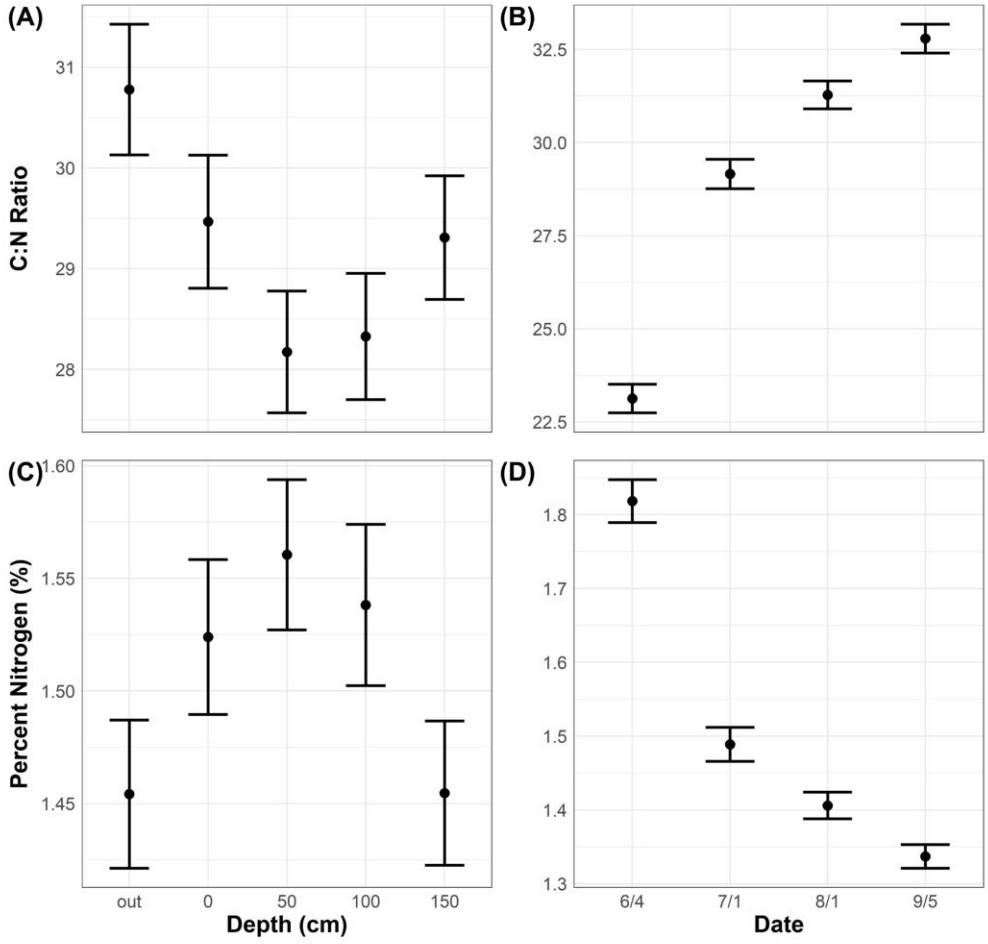

Figure 3.4. C:N ratio of leaves varying by depth (A) and date (B), and %N of leaves varying by depth (C) and date (D). Point and whiskers represent the mean ± standard error.

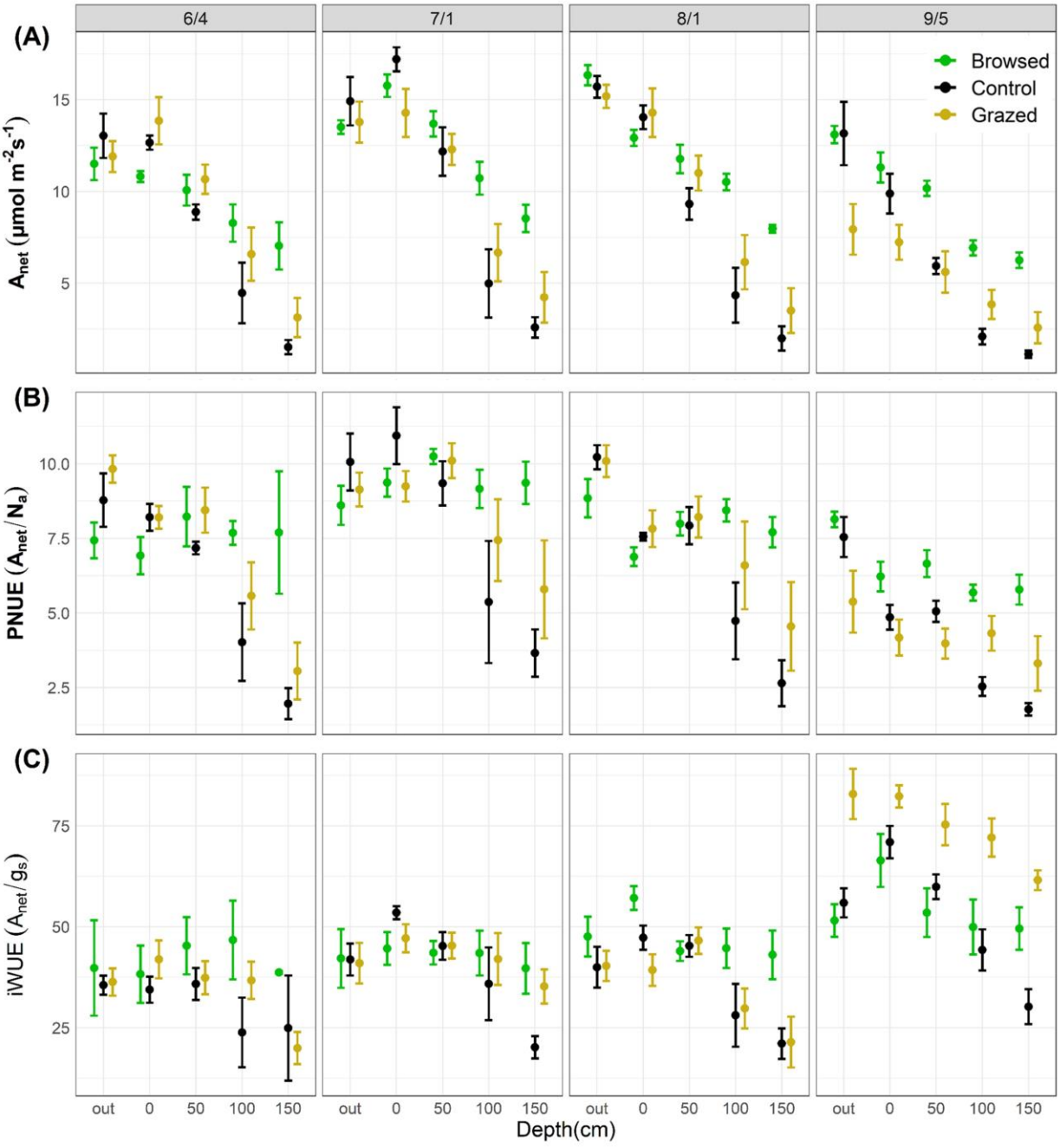

Figure 3.5. (A) Ambient photosynthetic rates, (B) photosynthetic nitrogen-use efficiency, and (C) intrinsic water-use efficiency of leaves in *C. drummondii* canopies varying by canopy position (out, 0 cm, 50 cm, 100 cm, and 150 cm), herbivory treatment (browsed, control, and grazed), and sampling period (6/4, 7/1, 8/1, 9/5). Point and whiskers represent the mean ± standard error.

Chapter 4 - Conclusion

Grasslands consist of roughly one third of the global terrestrial surface. They contain a large amount of the world's biodiversity, including a large proportion of the remaining megafauna (Chapin 2003, Suttie et al. 2005). Grasslands also play a central role to human civilization by sustaining livestock production for pastoral societies and ranchers around the world. Woody plant encroachment has led to a loss of grassland ecosystems worldwide and has had a significant impact on both biodiversity and livestock production. Mesic grasslands, such as the North American tallgrass prairie have been the most impacted by woody plant encroachment (Archer et al. 2017, Ratajczak et al. 2014). These grasslands contain the highest rates of woody plant encroachment in the Great Plains and the greatest potential to transition from grass dominated to woody dominated ecosystems due to their high precipitation (Staver et al. 2011, Ratajczak et al. 2014, Archer et al. 2017).

Dense canopies are a key factor contributing to the success of island forming clonal shrubs responsible for woody encroachment of mesic grasslands. By forming dense canopies, woody encroaching shrubs utilize reinforcing feedbacks that facilitate their encroachment throughout grasslands (Ratajczak et al. 2014, Staver et al. 2011). Dense canopies displace light intolerant C_4 grasses, resulting in fire extinction. Upon release from fires constraints, shrubs with clonal growth spread radially via belowground rhizomes, recruiting new ramets on their outer edge and increasing the area of the shrub island (Heisler et al. 2003, Briggs et al. 2005, McCarron et al. 2003). As these canopies get larger, the effectiveness of fire further decreases and hysteresis may occur, in which frequent fire is less capable of pushing the ecosystem back to a grassy state (Collins et al. 2021, Ratajczak et al. 2014). Despite the importance of dense canopies as a key driver of woody encroachment, very little is known about the mechanisms that

enable woody encroaching shrubs to achieve dense canopies. To fill this knowledge gap, I investigated the canopy structure and light environment in the canopies of *Cornus drummondii*, the predominant woody encroaching shrub in the Kansas tallgrass prairie, and the mechanisms enabling it to achieve these dense canopies.

In chapter 2, I investigated the vertical canopy structure and the behavior of light in canopies *C. drummondii*, and the effects of simulated browsing and grazing. In doing so, I also evaluated the accuracy of two indirect methods of measuring LAI against direct measurements to determine their accuracy in dense canopies of *C. drummondii*. Additionally, I also evaluate the effect of simulated browsing, and grazing on these factors. I took measurements of LAI, LAD, leaf inclination angle, and PAR across a vertical canopy gradient to evaluate the structure and quantity of light in canopies, and to make comparisons between direct and indirect measurements. I also calculated the coefficient of light extinction (*k*) and clumping index to better understand the relationship of light and foliage in canopy sections varying by depth and treatment, and to make comparisons between direct and indirect methods. My results indicated that the LAI of un-browsed canopies using direct methods averaged ~8.0 and distributed nearly half their LAI at the 50-100 cm canopy depth, making the LAD of this canopy section double the other canopy sections. The coefficient of light extinction (*k*) varied in response to LAD, resulting in differences in *k* by canopy depth and between treatments. The clumping index was greater at the 0-50 cm section compared to other sections, and greater in canopies of the browsed treatment compared to the other two treatments indicating that the ceptometer would overpredict LAI at the 0-50 cm depth and in the browsed treatment. LAI evaluated with the ceptometer was extremely accurate for control and grazed treatments, but overpredicted LAI in the browsed treatment by 46%, on average. Direct measurements using the 3D handheld scanner had a very strong

relationship with actual values but tended to overpredict LAI. My results highlight that the structure of *C. drummondii* canopies and the behavior of light in these canopies are not homogenous and vary by depth and treatment, which can affect the accuracy of indirect LAI measurements in the case of the simulated browsing treatment.

In chapter 3, I evaluated the vertical distribution of leaf traits and leaf physiology across canopies of *C. drummondii*, and their response to simulated browsing and grazing. I measured the canopy light availability (PAR), leaf level morphology (LMA), and nutrient allocation (N_a, C:N, %N) and their effects on leaf level physiology (J_{max}, Vc_{max}, A_{2000}, R_d, LCP), and integrative traits (A_{net}, PNUE, iWUE, $\delta^{13}C$). My results found that large vertical variation in LMA and N_a existed across canopies of *C. drummondii,* resulting in major differences in the physiological functioning of leaves. Leaves at the top of the canopy had high LMA and N_a leading to a high photosynthetic capacity, while leaves at the bottom of canopies had low LMA and maintained light compensation points (LCP) below ambient light levels despite having a lower apparent quantum yield. *C. drummondii* also modified its vertical allocation of leaf traits in response to browsing to facilitate a compensatory growth response. In response to greater light penetration in browsed canopies, LMA and N_a increased at lower canopy depths, leading to a greater photosynthetic capacity deeper in browsed canopies compared to control canopies. This response, along with greater light availability, facilitated greater photosynthesis and resource-use efficiency deeper in browsed canopies compared to control canopies.

Taken together, the results of this dissertation give a better understanding of the canopy structure of *C. drummondii,* and the mechanisms enabling *C. drummondii* to facilitate its dense canopy structure. The combination of high LAI, LAD, and intra-canopy leaf plasticity is a key driver of the success of *C. drummondii* for encroachment in the Kansas tallgrass prairie. High

intra-canopy leaf plasticity enables *C. drummondii* to maximize carbon gain of leaves across a greater range of light conditions. Not only does this result in greater carbon uptake for individual leaves across a wide range of light conditions, but it also enables *C. drummondii* to use a greater LAI to further increase carbon gain—since leaves can maintain positive photosynthetic rates across a greater range of light conditions. The large number of leaves maintaining positive photosynthetic rates in canopies of *C. drummondii* enables the rapid growth of clonal ramets on the edges of islands, enabling them to quickly develop dense canopies. The high LAI values of *C. drummondii* canopies enable it to shade out competitors to reduce fine fuel availability for fire. Along with this, the dense canopy structure (high LAD) of *C. drummondii* enables canopies to reach LAI values that displace grasses with less vertical growth, facilitating fire escape in shorter time periods than otherwise possible. The combination of traits exhibited by canopies of *C. drummondii* (high LAI, LAD, and leaf plasticity), along with a compensatory growth response to browsing are key mechanisms contributing to the success of *C. drummondii* and potentially other species responsible for grassland woody encroachment.

References

Archer SR, Andersen EM, Predick KI, Schwinning S, Steidl RJ, Woods SR (2017) Woody plant encroachment: causes and consequences. In *Rangeland systems* (pp. 25-84). Springer, Cham.

Briggs JM, Knapp AK, Blair JM, Heisler JL, Hoch GA, Lett MS, McCarron JK (2005) An ecosystem in transition: causes and consequences of the conversion of mesic grassland to shrubland. BioScience 55:243-54.Chapin III FS (2003) Effects of plant traits on ecosystem and regional processes: a conceptual framework for predicting the consequences of global change. Annals of botany 91:455-63.

Collins SL, Nippert JB, Blair JM, Briggs JM, Blackmore P, Ratajczak Z (2021) Fire frequency, state change and hysteresis in tallgrass prairie. Ecology Letters 24:636-47.

Heisler JL, Briggs JM, Knapp AK. (2003) Long-term patterns of shrub expansion in a C4 - dominated grassland: Fire frequency and the dynamics of shrub cover and abundance. American Journal of Botany 90:423–428.

McCarron JK, Knapp AK (2003) C3 shrub expansion in a C4 grassland: positive post-fire responses in resources and shoot growth. American Journal of Botany 90:1496-501.

Ratajczak, Z., Nippert, J. B., & Ocheltree, T. W. (2014). Abrupt transition of mesic grassland to shrubland: evidence for thresholds, alternative attractors, and regime shifts. Ecology 95: 2633–2645.

Staver AC, Archibald S, Levin SA (2011) The global extent and determinants of savanna and forest as alternative biome states. Science 334:230-2.

Suttie JM, Reynolds SG, Batello C (2005) Grasslands of the world. Food and Agriculture Organization of the United Nations, Rome.

Appendix A - Additional Information

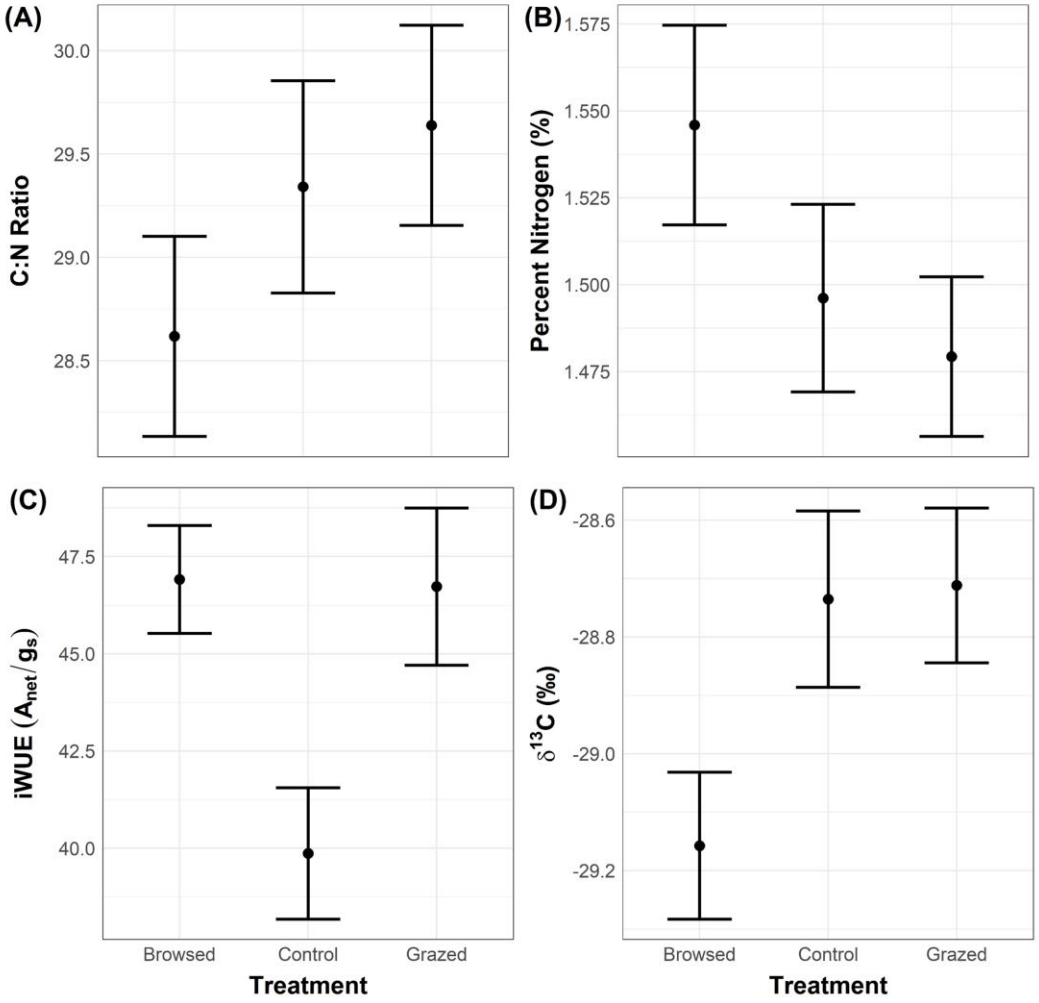

Figure A.1. C:N ratio of leaves varying by treatment, (B) %N of leaves varying by treatment, (C) iWUE of leaves varying by treatment, and (D) leaf $\delta^{13}C$ varying by treatment. Point and whiskers represent the mean ± standard error.

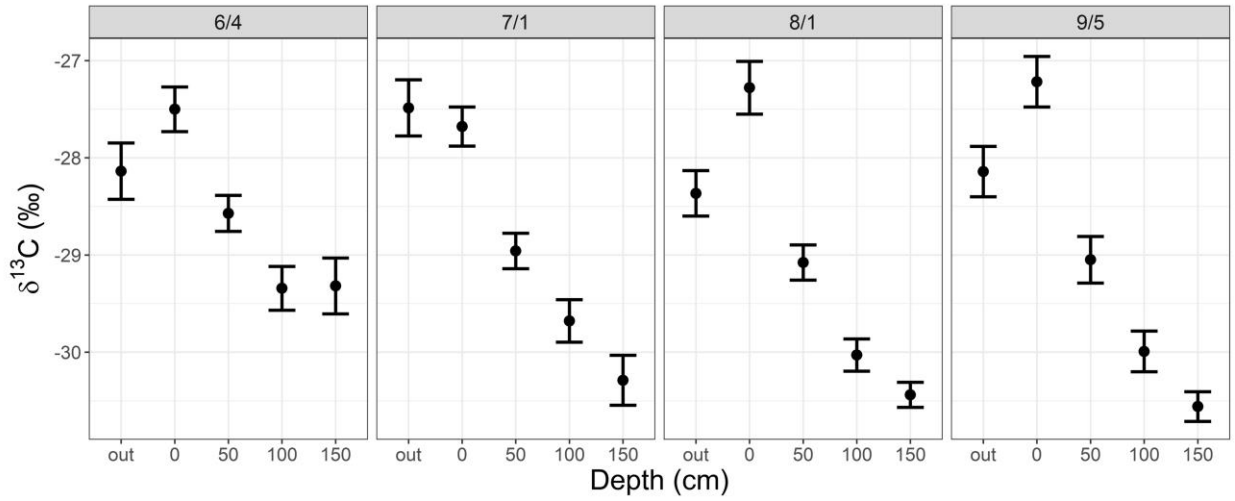

Figure A.2. $\delta^{13}C$ of leaves in *C. drummondii* canopies varying by canopy position (out, 0 cm, 50 cm, 100 cm, and 150 cm) and sampling period (6/4/, 7/1, 8/1, 9/5). Point and whiskers represent the mean ± standard error.

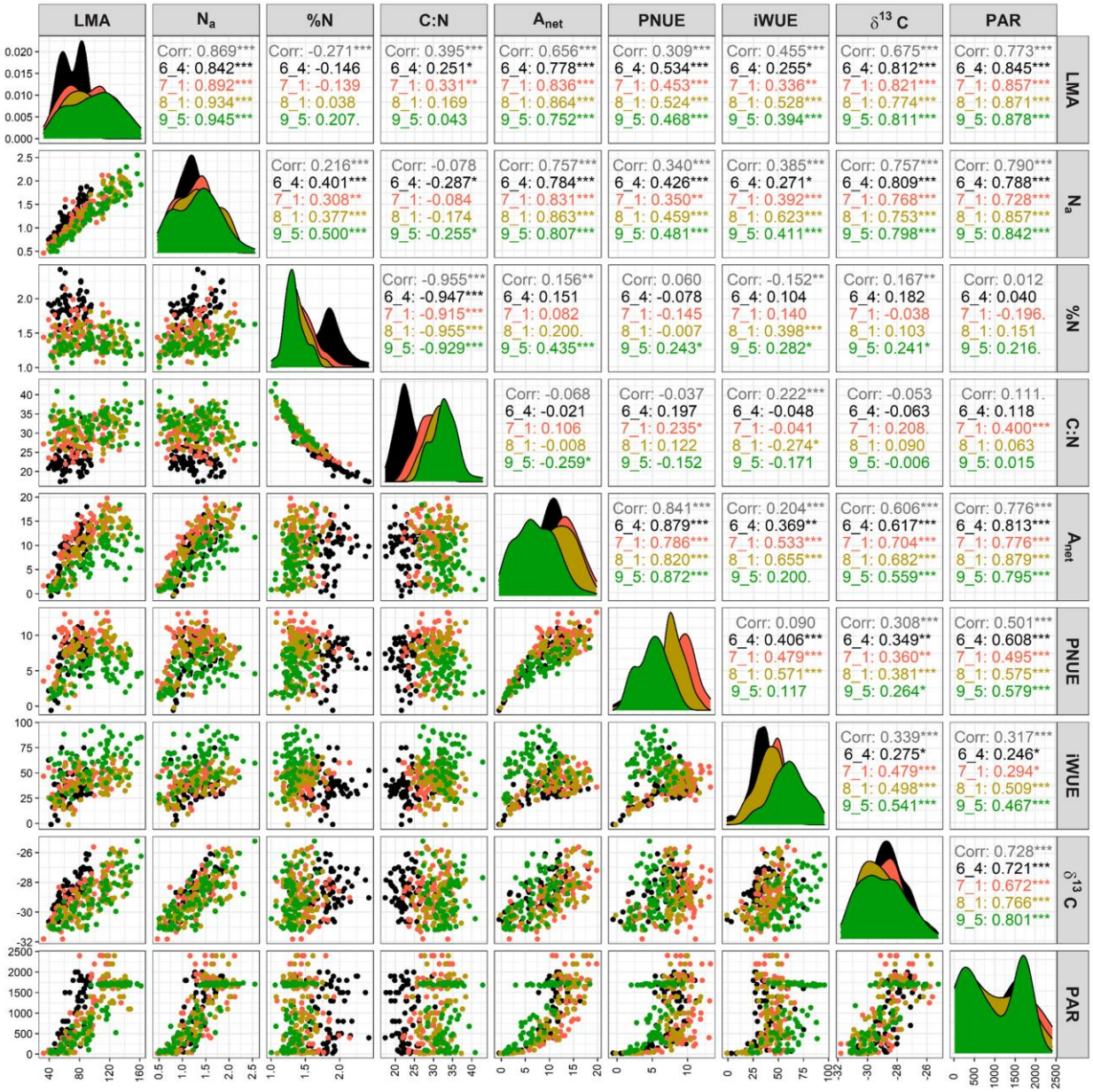

Figure A.3. Pearsons matrices for leaf morphological and physiological parameters sampled across the growing season. For each bivariate comparison, pearsons correlation coefficients (r) are given for the entire growing season (grey), the 6/4 sampling period (black), the 7/1 sampling period (red), the 8/1 sampling period (gold/yellow), and the 9/5 sampling period (green). Correlations with P-values < 0.05 are represented by an asterisk (*), P-value < 0.01 are represented by two asterisks (**), and P-values < 0.001 are represented by three asterisks (***).

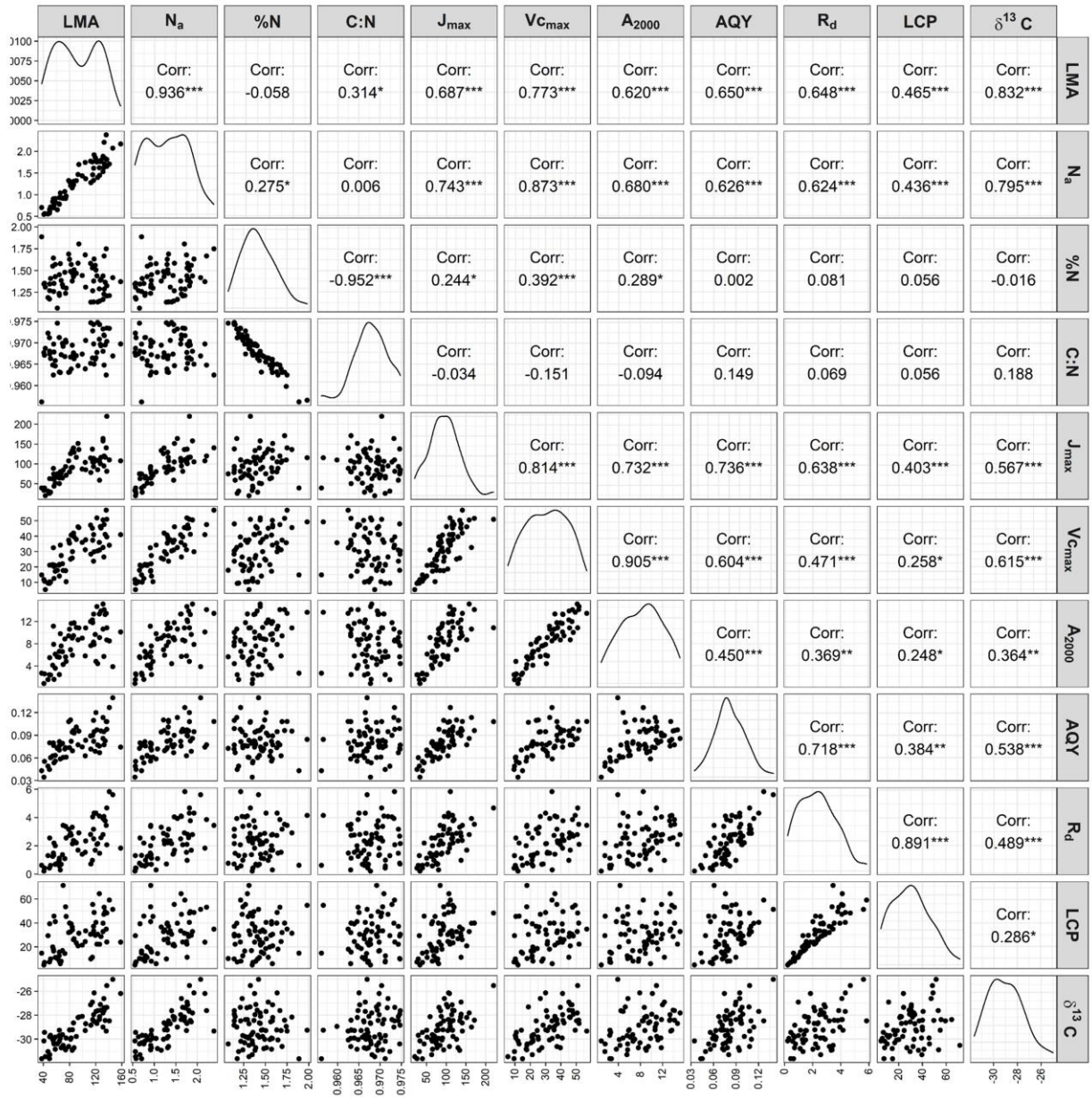

Figure A.4. Pearsons matrices for leaf morphological parameters from leaves used in the *A*-c_i and light response curves, and physiological parameters derived from the *A*-c_i and light response curves. Correlatiosn with P-values < 0.05 are represented by an asterisk (*), P-value < 0.01 are represented by two asterisks (**), and P-values< 0.001 are represented by three asterisks (***).